Placenta to cartilage: direct conversion of human placenta to chondrocytes with transformation by defined factors

Ryuga Ishii[a,b,*], Daisuke Kami[a,c,*], Masashi Toyoda[a,c], Hatsune Makino[a], Satoshi Gojo[c], Toshiharu Ishii[b], and Akihiro Umezawa[a]

[a]Department of Reproductive Biology and Pathology, National Research Institute for Child Health and Development, Tokyo 157-8535, Japan; [b]Department of Pathology, Toho University School of Medicine, Tokyo 143-8540, Japan; [c]Tokyo Metropolitan Geriatric Hospital and Institute of Gerontology, Tokyo 173-0015, Japan

ABSTRACT **Cellular differentiation and lineage commitment are considered to be robust and irreversible processes during development. Recent work has shown that mouse and human fibroblasts can be reprogrammed to a pluripotent state with a combination of four transcription factors. We hypothesized that combinatorial expression of chondrocyte-specific transcription factors could directly convert human placental cells into chondrocytes. Starting from a pool of candidate genes, we identified a combination of only five genes (5F pool)—*BCL6*, *T* (also called *BRACHYURY*), *c-MYC*, *MITF*, and *BAF60C* (also called *SMARCD3*)—that rapidly and efficiently convert postnatal human chorion and decidual cells into chondrocytes. The cells generated expressed multiple cartilage-specific genes, such as *Collagen type II α1*, *LINK PROTEIN-1*, and *AGGRECAN*, and exhibited characteristics of cartilage both in vivo and in vitro. Expression of the endogenous genes for *T* and *MITF* was initiated, implying that the cell conversion is due to not only the forced expression of the transgenes, but also to cellular reprogramming by the transgenes. This direct conversion system from noncartilage tissue to cartilaginous tissue is a substantial advance toward understanding cartilage development, cell-based therapy, and oncogenesis of chondrocytes.**

Monitoring Editor
Elly Tanaka
Technical University Dresden

Received: Oct 18, 2011
Revised: Jul 12, 2012
Accepted: Jul 20, 2012

INTRODUCTION

The possibility of redirecting cell differentiation by overexpression of genes was suggested by H. Weintraub with the identification of the "master gene," *MyoD* (Davis *et al.*, 1987). The process was believed to involve reversion to a less differentiated state, a kind of dedifferentiation, before the new cell type is formed. Another process has since been introduced—the concept of direct conversion or direct reprogramming without dedifferentiation. This process is believed to be direct lineage switching rather than lineage switching back to a branch point and out again in a different direction (Hochedlinger and Jaenisch, 2006; Orkin and Zon, 2008). Direct conversion has been shown in β cells, cardiomyocytes, and neurons. A specific combination of three transcription factors (*Ngn3*, *Pdx1*, and *MafA*) reprograms differentiates pancreatic exocrine cells in adult mice into cells that closely resemble β cells (Zhou *et al.*, 2008); a combination of three factors (*Gata4*, *Tbx5*, and *Baf60c*) induces noncardiac mesoderm to differentiate directly into contractile cardiomyocytes (Ieda *et al.*, 2010); and a combination of three factors (*Ascl1*, *Brn2*, and *Myt1l*) converts mouse fibroblasts into functional neurons (Vierbuchen *et al.*, 2010). In this study, we used the strategy of direct conversion to generate chondrocytes from human somatic cells.

During skeletal development, chondrogenesis starts from condensed mesenchyme tissue, which differentiates into chondrocytes and begins secreting the molecules that form the extracellular matrix and leads to endochondral ossification. Cartilage is a stiff yet flexible connective tissue found in many areas in the bodies of humans and other animals. It is composed of chondrocytes, which

This article was published online ahead of print in MBoC in Press (http://www.molbiolcell.org/cgi/doi/10.1091/mbc.E11-10-0869) on July 25, 2012.

*These authors contributed equally to this study.

Address correspondence to: Akihiro Umezawa (umezawa@1985.jukuin.keio.ac.jp).

Abbreviations used: *ACAN*, *AGGRECAN*; *COL2A1*, *Collagen Type II α1*; *COL10A1*, *Collagen Type X α1*; *CRTL1*, *LINK PROTEIN-1*; GAPDH, glyceraldehyde-3-phosphate dehydrogenase; HE, hematoxylin and eosin; iCS, induced chondrosarcoma; MEFs, mouse embryonic fibroblasts; PCA, principal component analysis; PDs, population doublings; RT-PCR, reverse transcriptase PCR; siRNA, small interfering RNA; STRs, short tandem repeats.

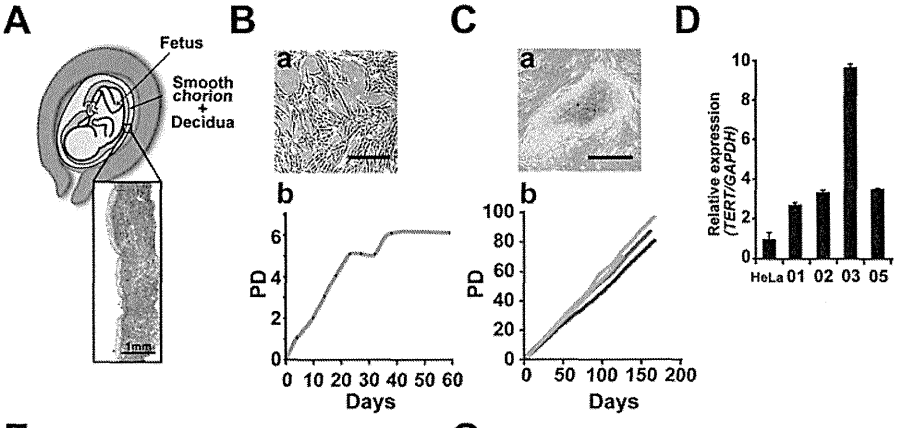

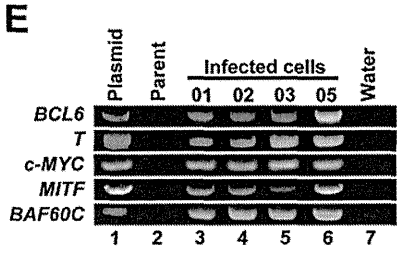

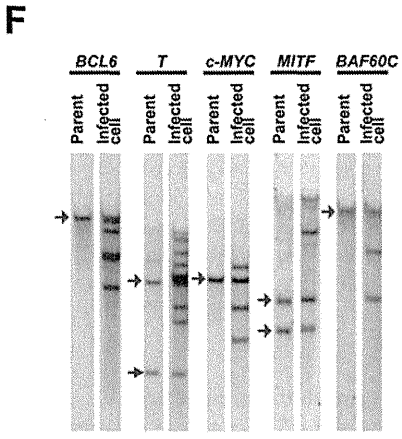

G

Locus	Parent		01		02		03	
D3S1358	15		15		15		15	
TH01	6		6		6		6	
D21S11	30	31.2	30	31.2	30	31.2	30	31.2
D18S51	14		14		14		14	
Penta_E	14	21	14	21	14	21	14	21
D5S818	10	11	10	11	10	11	10	11
D13S317	11		11		11		11	
D7S820	8	11	8	11	8	11	8	11
D16S539	12	13	12	13	12	13	12	13
CSF1PO	11	12	11	12	11	12	11	12
Penta_D	10	12	10	12	10	12	10	12
AMEL	X		X		X		X	
vWA	16		16		16		16	
D8S1179	10	13	10	13	10	13	10	13
TPOX	8	11	8	11	8	11	8	11
FGA	22	26	22	26	22	26	22	26

Locus	Parent		05	
D3S1358	15	16	15	16
TH01	6	9.3	6	9.3
D21S11	30	31.2	30	31.2
D18S51	14	19	14	19
Penta_E	15	21	15	21
D5S818	10		10	
D13S317	12		12	
D7S820	8	12	8	12
D16S539	9	12	9	12
CSF1PO	11	12	11	12
Penta_D	12		12	
AMEL	X	Y	X	Y
vWA	14	16	14	16
D8S1179	10	13	10	13
TPOX	11		11	
FGA	19	22	19	22

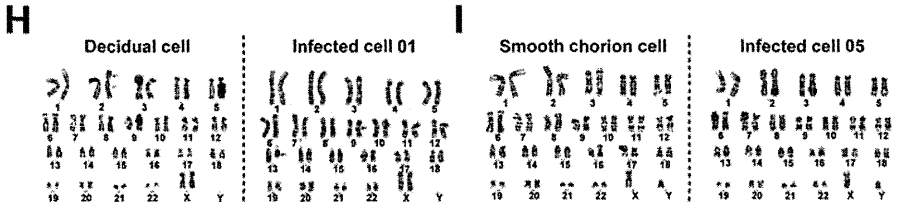

FIGURE 1: Characterization of infected cells. (A) Cell source for infection. Smooth chorion- and decidua-derived cells were used to investigate chondrogenesis by direct reprogramming. Bars, 1 mm. (B) Cell cultivation. (a) Phase contrast micrograph of parental cells. Bars indicate 200 μm. (b) Growth curve of parental cells. (C) Cells infected with five genes. (a) Phase contrast micrograph of infected cells. Bars, 200 μm. (b) Growth curve of infected cells. Orange, clone 01; red, clone 02; blue, clone 03; green, clone 05. Vertical axis indicates population doublings (PDs), and horizontal axis indicates days after infection. (D) Quantitative RT-PCR of *TERT* expression in the infected cell lines (clones 01, 02, 03, and 05). Individual RNA expression levels were normalized to respective *GAPDH* expression levels. HeLa cells were used for reference. Error bars, SD ($n = 3$). (E) Genomic DNA PCR analysis of uninfected and infected cells. To investigate chromosomal integration of the genes by retroviral infection, we performed genomic DNA PCR analysis, using transgene-specific primers of each gene. Five transgenes (*BCL6*, *T*, *c-MYC*, *MITF*, and *BAF60C*) were detected in all of the infected cell lines. (F) Southern blot analyses of the infected cells (clone 01). Genomic DNA was digested with *Spe*I, *Mfe*I, *Bgl*II, *Nco*I, and *Bam*HI and then probed for probes of the genes for *BCL6*, *T*, *c-MYC*, *MITF*, and *BAF60C*, respectively. The transgenes (*BCL6*, *T*, *c-MYC*, *MITF*, and *BAF60C*) were detected in all of the infected cell lines. Arrows indicate bands corresponding to the endogenous genes. (G) STR analysis of parental cells and the infected cells. All of the infected cells exhibited the same STR patterns as parental cells. (H) G-band chromosome analysis for parental cells with XX chromosomes and infected cells 01. (I) G-band chromosome analysis for parental cells with XY chromosomes and infected cells 05.

produce a large amount of collagen fiber, an abundant ground substance rich in proteoglycans, and elastin fibers. Developmentally, the undifferentiated mesenchymal cells migrate into the limb field and condense to form the cartilage anlage. Bone morphogenic proteins and transforming growth factor-β initiate the chondrogenic program and have significant effects on chondrogenesis through distinct mechanisms in a stage-specific manner. In addition to soluble factors, the high mobility group–domain transcription factors such as *Sox5*, *Sox6*, and *Sox9* control chondrogenic differentiation, maintain the chondrocyte phenotype, and regulate expression of extracellular matrix molecules, such as cartilage-specific collagen type II (Lefebvre *et al.*, 1997).

Murine chondrocytes can be converted from fetal fibroblasts by the direct reprogramming method using the cartilage-specific transcription factors *Sox9*, *c-Myc*, and *Klf4* (Hiramatsu *et al.*, 2011), but human chondrocytes converted from different types of cells have not yet been reported. In the present study, we generated chondrosarcoma cell lines derived from human placenta by the direct reprogramming method, using a different set of genes. Placental membrane can be obtained at every delivery and is usually discarded. Therefore it is an easily accessible cellular source without ethical problems.

RESULTS

Isolation of cells from smooth chorion and decidua

We used smooth chorion and decidua for a cell source by removing the amnion from the placental membrane and used the explant culture method in which the cells are outgrown from pieces of smooth chorion and decidua attached to dishes (Figure 1A and Supplemental Figure S1). The adherent chorion- and decidua-derived cells were passaged when the cells reached ~80% confluence. These placenta-derived cells continued to grow for 30 d, which was five population doublings (PDs), before reaching senescence (Figure 1B). The cells at four PDs were used as "parental cells" for conversion analysis.

Infection of transcription factors into placenta-derived cells

To select candidates for transcription factors that would be required to reprogram fibroblasts to a cartilage fate, we used microarray analyses to identify transcription factors and chromatin remodeling factors with greater expression in mouse embryonic stem cell that are differentiated into mesoderm. We started with a 14-gene set, that is, genes for mesoderm-specific transcription factors (*T*, *MITF*, *TBX5*, *TBX20*, *CSX/NKX2.5*, *GATA4*, *MEF2C*, *MESP1*, *ISL1*, *BCL6*, and *PRDM16*) and chromatin-remodeling/reprogramming factors (*BAF60C*, *c-MYC*, and *KLF4*). We generated individual retroviruses to efficiently express each gene. Viral infections were preceded by transfection of small interfering RNA (siRNA) to the *p53* gene (Supplemental Figure S2). Parallel experiments using retrovirus carrying the EGFP gene indicated that infection efficiency was nearly 100%. We investigated expression of cartilage-associated genes such as *Collagen Type II α1* (*COL2A1*), *Collagen Type X α1* (*COL10A1*), *LINK PROTEIN-1* (*CRTL1*), and *AGGRECAN* (*ACAN*) by reverse transcriptase (RT)-PCR and identified five genes (*BCL6*, *T*, *c-MYC*, *MITF*, and *BAF60C*) that induced chondrocyte gene expression. The induction levels of the cartilage-associated genes were greatly reduced by elimination of any one gene from the five-gene set. We thus decided to use the five-gene set for chondrogenic induction for subsequent experiments. After we seeded infected cells on mouse embryonic fibroblasts (MEFs), we detected a very large number of mouse embryonic stem cell–like colonies on MEFs 15 d after infection of the 5F pool (Figure 1C, a). Efficiency of colony formation (colony number per the number of cells infected) was 5.76 (±0.21) × 10^{-4}. We randomly picked four clones and analyzed cell growth rates. The cells replicated at a rate of once every 2 d and continued to grow for >150 d without reaching senescence (Figure 1C, b). All four clones expressed the *TERT* gene after establishment as a cell line (Figure 1D). The cells infected with the five genes exhibited a chondrogenic phenotype with malignant transformation, as shown by following results, and were thus designated induced chondrosarcoma (iCS) cells.

To determine chromosomal insertion of the genes, we performed genomic DNA PCR analysis (Figure 1E). The genes encoding BCL6, T, c-MYC, MITF, and BAF60C were detected in chromosomal genome of the four clones. Southern blot analysis with cDNA probes of each of the five genes (*BCL6*, *T*, *c-MYC*, *MITF*, and *BAF60C*) confirmed that each clone had chromosomal integration of the exogenously infected genes (Figure 1F and Supplemental Figure S3). The analysis of the 16 short tandem repeats (STRs) revealed that the infected clones were derived from parental cells: clones 1, 2 and 3 were derived from parental cells of the same donor with XX chromosomes, and clone 5 was derived from different parental cells with XY chromosome (Figure 1G). The STR patterns of the infected cells differed from those of any cell lines deposited on National Institutes of Health website (http://stemcells.nih.gov/research/nihresearch/scunit/genotyping.htm), implying that the cells generated are not a contamination of previously established cell lines. To determine the karyotypes of the iCS cell lines, karyotypic analysis was performed at different passages (P6– P23). Chromosomal G-band analyses showed that each clone had a normal karyotype with 46XX and 46XY (Figure 1, H and I, respectively). We then performed karyotypic analysis on iCS clones after prolonged passages (P15 and P23 for iCS-01; P13 and P21 for iCS-02; P12 and P21 for iCS-03; P7 and P23 for iCS-05, and did not detect any significant karyotypic change (Supplemental Figure S4).

In vitro chondrogenic phenotypes of the cells infected with the 5F pool

To investigate whether the infected cells exhibit a chondrogenic phenotype in vitro, we performed RT-PCR analysis using primers of the cartilage-specific genes (Figure 2A and Supplemental Table S1; Sekiya *et al.*, 2002; Shirasawa *et al.*, 2006). All the cell lines expressed the chondrocyte-specific/associated transcription factors (*SOX5*, *SOX6*, and *SOX9*), structural genes (*COL1A1*, *COL2A1*, *CRTL1*, and *ACAN*), and immortalizing gene (*TERT*). To see whether the endogenous genes for *BCL6*, *T*, *c-MYC*, *MITF*, and *BAF60C* were expressed by reprogramming, we performed RT-PCR analysis by the primers specific to the endogenous gene but not the transgenes (Supplemental Figure S5). Endogenous genes such as *T*, *MITF*, and *BAF60C* were induced (Figure 2B). To determine the surface markers of the cells, we performed flow cytometric analysis. All clones were positive for CD44, CD49c, CD151, and CD166 but not CD117 and CD133, suggesting that the cell marker pattern of iCS cells is compatible with that of chondrocytes (Figure 2C; Grogan *et al.*, 2007). Western blot analysis revealed that all the infected cells expressed COL2A1 and COL1A1 at the protein level (Figure 2D and Supplemental Figure S6). Comprehensive gene expression analysis showed that the expression pattern of the infected cells is similar to that of human adult chondrocytes and human fetal chondrocytes (Figure 2E). Expression of cartilage-specific genes such as *Sox9*, *Aggrecan*, and *Matrix Gla-protein* was detected in the infected cells and chondrocytes but not in the parent human smooth chorion and decidua cells (Figure 2F). Conversely, expression of placenta-associated genes such as *GATA3*, *CD200*, *PDCD1LG2*, *OLR1*, *TEK*, *HSD17B2*, and *FOXF1* was lost in the infected cells. Hierarchical clustering analysis revealed that the infected cells were grouped into the same category that includes chondrocytes obtained from human fetuses and adults (Figure 2G). In addition, principal component analysis (PCA) revealed that the infected cells and chondrocytes showed similar scores in the PC2 axis (Figure 2H). The representative genes (principal components) of the PC2 axis in Table 1 include cartilage-specific genes such as *Aggrecan*, *Fibromodulin*, and *Matrix Gla-protein* (Plaas and Wong-Palms, 1993; Yagami *et al.*, 1999; Sekiya *et al.*, 2002; Hjorten *et al.*, 2007; Surmann-Schmitt *et al.*, 2009).

Inhibition of five factors by small interfering RNA

To investigate the involvement of the five factors in chondrogenesis, we suppressed their expression by siRNA (Supplemental Table S2). The mRNAs for the five factors (*BCL6*, *T*, *c-MYC*, *MITF*, and *BAF60C*) were significantly decreased by siRNAs compared with control cells transfected with control siRNAs (Figure 3, A and B, and Supplemental Figures S7–S9). Morphological changes in the siRNA-treated cells were too variable to interpret. Gene expression of the chondrogenic-specific/associated transcription factors (*SOX5*, *SOX6*, and *SOX9*) and structural genes (*COL1A1*, *COL2A1*, *CRTL1*, and *ACAN*) decreased significantly in si*T* (siRNA to the *T* gene)-transfected cells compared with cells treated with control siRNA (Figure 3C and Supplemental Figure S10), suggesting that *T* is necessary for chondrogenic conversion (Hoffmann *et al.*, 2002). In addition, expression of the genes for *SOX5*, *SOX6*, *COL1A1*, and *COL2A1* decreased significantly in si*MITF*-transfected cells compared with cells transfected with control siRNA, suggesting that *MITF* is also necessary for chondrogenic conversion. In contrast, treatment of siRNA to *BCL6*, *c-MYC*, and *BAF60C*) did not alter cartilage-related genes (Zelzer and Olsen, 2003; Levy and Fisher, 2011). si*MITF* diminished the cobblestone appearance of iCS colonies and the cell lining at the periphery of iCS colonies and altered the appearance of the iCS cells to a fibroblast-like morphology, which may be related to decreased expression of the cartilage-associated genes.

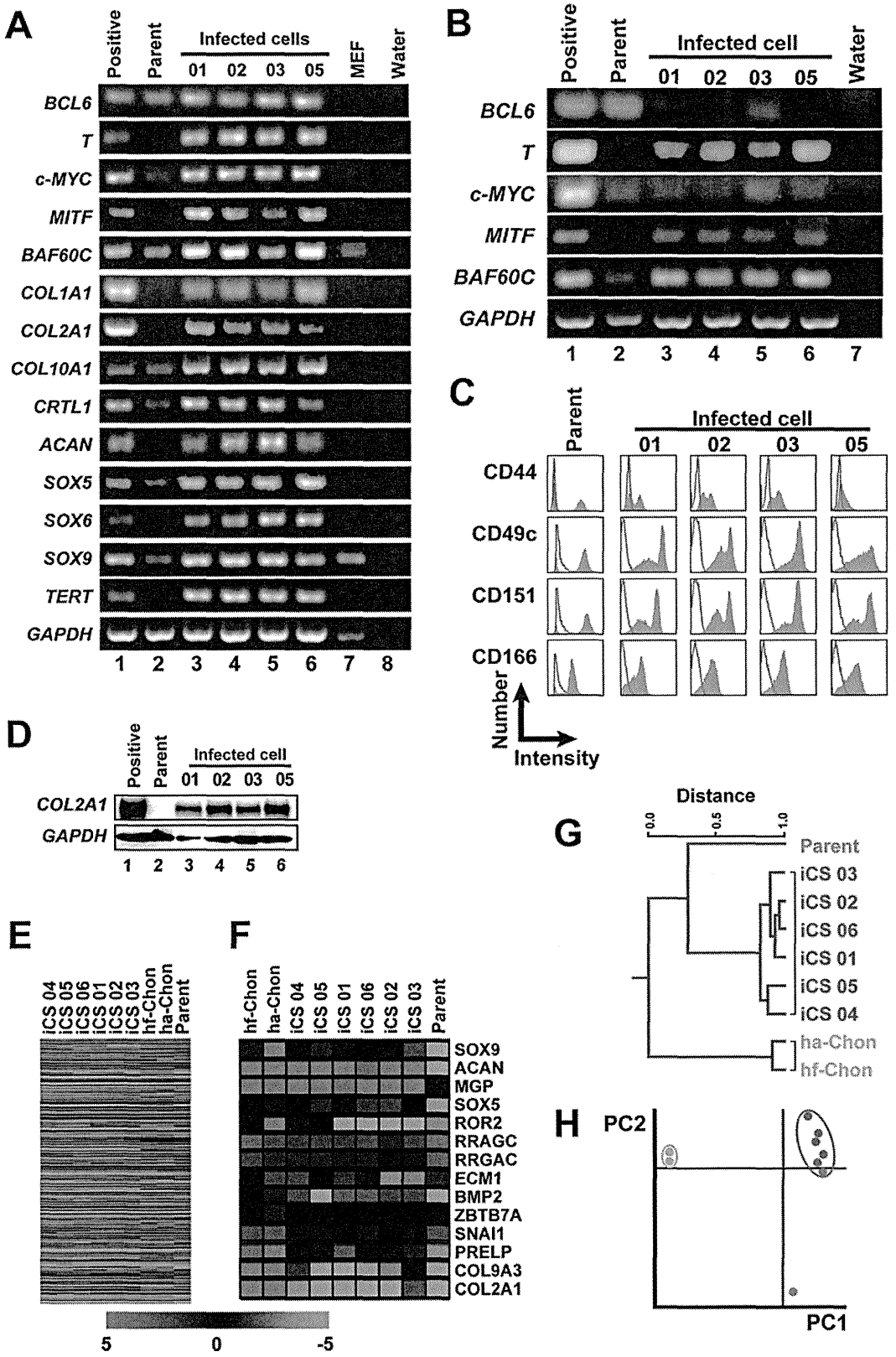

FIGURE 2: Chondrogenic phenotypes of infected cells. (A) RT-PCR analysis of the genes encoding cartilage-specific proteins (SOX5, SOX6, SOX9, COL1A1, COL2A1, COL10A1, CRTL1, and ACAN), immortalizing gene (TERT), and the infected genes (BCL6, T, c-MYC, MITF, and BAF60C). Primers that detect both the transgenes and endogenous genes for BCL6, T, c-MYC, MITF, and BAF60C were used (Supplemental Figure S5C). RNAs from the following sources were used for positive controls: heart for BCL6, MITF, BAF60C, and GAPDH; iPS cells for T, c-MYC, and TERT; and cartilage for COL1A1, COL2A1, COL10A1, CRTL1, ACAN, SOX5, SOX6, and SOX9. H_2O (water without RNA) served as a

Gene symbol	Description	Gene symbol	Description
ACAN	Aggrecan	CLEC4D	C-type lectin domain family 4, member D
FMOD	Fibromodulin	NRAP	Nebulin-related anchoring protein
MGP	Matrix Gla protein	OR2V2	Olfactory receptor, family 2, subfamily V, member 2
LRRC48	Leucine-rich repeat containing 48	KCNH7	Potassium voltage-gated channel, subfamily H (eag-related), member 7
SLPI	Secretory leukocyte peptidase inhibitor	KCNK17	Potassium channel, subfamily K, member 17
RAB11FIP4	RAB11 family interacting protein 4 (class II)	DRD1	Dopamine receptor D1
TLR5	Toll-like receptor 5	CTNNA2	Catenin (cadherin-associated protein), α2
NEBL	Nebulette	FMR1NB	Fragile X mental retardation 1 neighbor
RAB11FIP4	RAB11 family interacting protein 4 (class II)	ABCC12	ATP-binding cassette, subfamily C (CFTR/MRP), member 12
CAPG	Capping protein (actin filament), gelsolin-like	SLITRK3	SLIT and NTRK-like family, member 3
SLC26A4	Solute carrier family 26, member 4	CIITA	Class II, major histocompatibility complex, transactivator
MIF	Macrophage migration inhibitory factor (glycosylation-inhibiting factor)	GP2	Glycoprotein 2 (zymogen granule membrane)
CALR3	Calreticulin 3	OR12D3	Olfactory receptor, family 12, subfamily D, member 3
ESPN	Espin	GALNTL4	UDP-*N*-acetyl-α-D-galactosamine
SLC7A2	Solute carrier family 7 (cationic amino acid transporter, y+ system), member 2	BRSK2	BR serine/threonine kinase 2
CHRNA4	Cholinergic receptor, nicotinic, α4	L08961	Transmembrane tyrosine kinase mRNA
ZBTB10	Zinc finger and BTB–domain containing 10	RAB33B	RAB33B, member RAS oncogene family
ND3	NADH-ubiquinone oxidoreductase chain 3(NADH dehydrogenase subunit 3)	ELA1	Elastase 1, pancreatic
EFNA1	Ephrin-A1	ASPA	Aspartoacylase (Canavan disease)
RGMA	RGM domain family, member A	IL18RAP	Interleukin 18 receptor accessory protein
ENST00000390243	Immunoglobulin κ light-chain V gene segment	EPHA8	EPH receptor A8
GPA33	Glycoprotein A33 (transmembrane)	CXCR6	Chemokine (C-X-C motif) receptor 6
CLMN	Calmin (calponin-like, transmembrane)	BAGE	B melanoma antigen
RAB11FIP4	RAB11 family interacting protein 4 (class II)	SIRPG	Signal-regulatory protein γ
KRT26	Keratin 26	AF083118	CATX-2 mRNA
YBX2	Y box–binding protein 2	TSPAN16	Tetraspanin 16
EEF1G	Eukaryotic translation elongation factor 1 γ	AF028840	Kruppel-associated box protein mRNA
NAG18	NAG18 protein on chromosome 19	WIF1	WNT inhibitory factor 1
CX62	Connexin 62	TTTY9A	Testis-specific transcript, Y-linked 9A (TTTY9A) on chromosome Y
KCNC2	Potassium voltage-gated channel, Shaw-related subfamily, member 2	LRRC50	Leucine-rich repeat containing 50
TSPAN33	Tetraspanin 33	ENST0000037416	Collagen, type XXVII, α1
PTCH1	Patched homologue 1 (*Drosophila*)	WFDC12	WAP four-disulfide c ore domain 12
DEFB126	Defensin, β126		
RAMP3	Receptor (G protein–coupled) activity–modifying protein 3		

TABLE 1: Representative genes in PC2 axis of the PCA.

negative control. (B) RT-PCR analysis of the endogenous genes encoding T, MITF, and BAF60C. The primers were prepared to amplify the endogenous genes but not the transgenes. RNAs from the following sources were used for positive controls: heart for BCL6, MITF, BAF60C, and GAPDH; and iPS cells for T and c-MYC. H_2O (water without RNA) served as a negative control. (C) Flow cytometric analysis of cell surface markers on the parental cells and infected cells. All of the results were compared with each isotype control. The *X*- and *Y*-axes indicate the intensity and the cell number, respectively. (D) Western blot analysis of COL2A1 protein in the infected cells and parental cells. (E, F) The heat map in the infected cells and parental cells. Each row represents a gene; each column represents a cell population. Expression levels of representative genes are shown in F. (G) Hierarchical clustering analysis (TIGR MeV; see *Materials and Methods*), based on expression levels of the cartilage-associated genes. (H) Principal component analysis of gene expression levels.

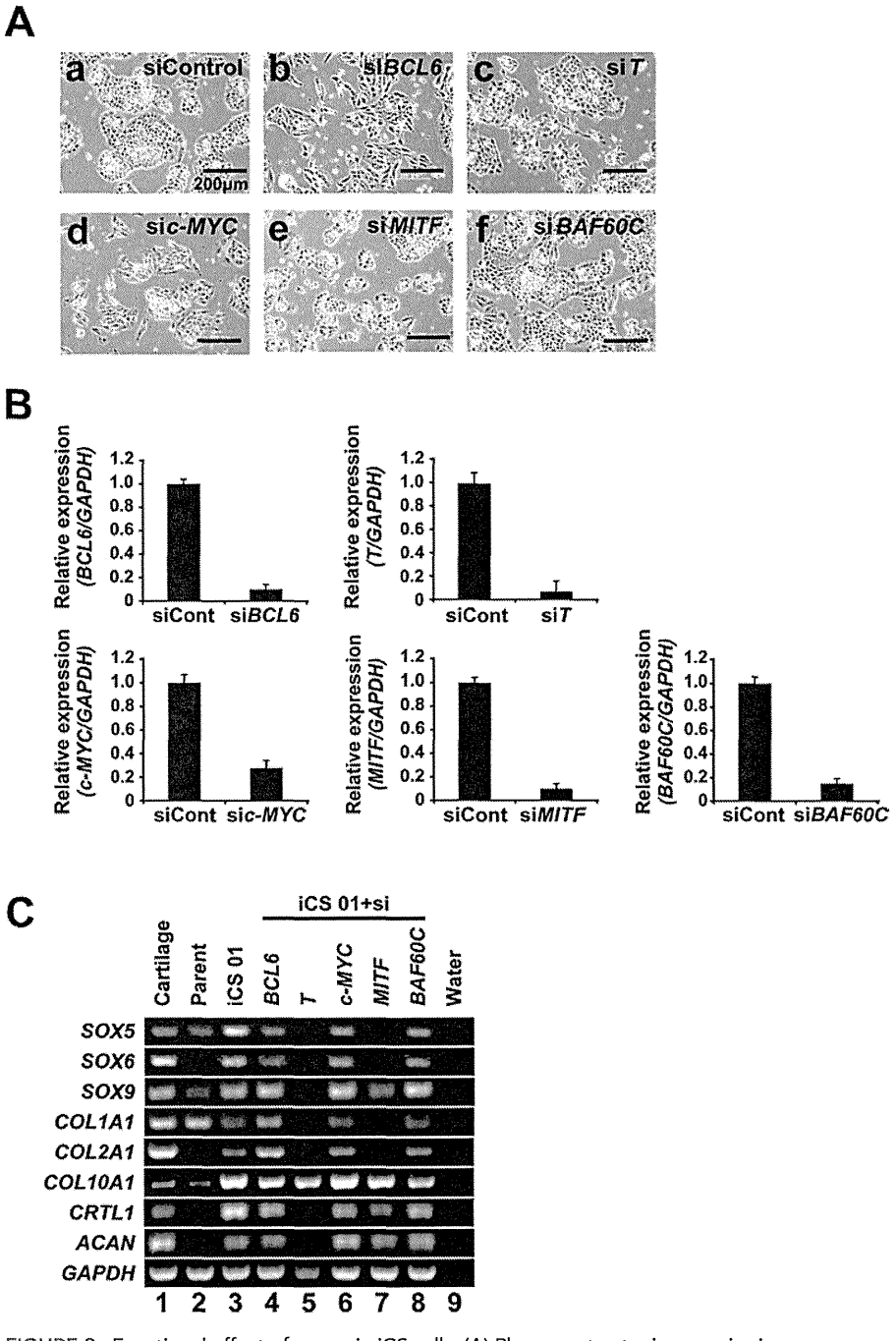

FIGURE 3: Functional effect of genes in iCS cells. (A) Phase contrast microscopic views. (a) Control siRNA–treated iCS cells. (b) *BCL6* siRNA–treated iCS cells. (c) *T* siRNA–treated iCS cells. (d) *c-MYC* siRNA–treated iCS cells. (e) *MITF* siRNA–treated iCS cells. (f) *BAF60C* siRNA–treated iCS cells. Bars, 200 μm. (B) Quantitative RT-PCR of each gene in siRNA-treated cells. Individual RNA expression levels were normalized to respective *GAPDH* expression levels. Error bars, mean ± SD ($n = 3$). (C) RT-PCR analysis of the genes encoding SOX5, SOX6, SOX9, COL1A1, COL2A1, COL10A1, CRTL1, and ACAN. Human cartilage and H_2O (water without RNA) served as positive and negative controls, respectively.

Cartilage formation after implantation of the cells infected with the 5F pool

To investigate whether iCS cells exhibit a chondrogenic phenotype in vivo, we intradermally injected the cells into dorsal flanks of immunodeficient Balb/c nu/nu mice. The masses generated underwent histopathological analysis 7 wk after injection. The injected cells generated cartilage that exhibited metachromasia by toluidine blue staining and were light blue when stained with Alcian blue (Figure 4A). In contrast, implantation of parental cells produced neither tumor nor cartilage (Figure 4E). RT-PCR analysis showed that iCS cartilage expressed genes for *COL1A1*, *COL2A1*, *COL10A1*, *CRTL1*, *ACAN*, CD44, CD49c, CD151, and CD166 (Figure 4B). Western blot analysis showed that iCS cartilage produced collagen type II at the protein level (Figure 4C). We also performed immunohistochemical analysis using antibodies to vimentin, collagen type II, and Ki-67. The antibody for vimentin that we used specifically reacts with human protein but not murine protein. The antibody for Ki-67 reacts with a human nuclear cell proliferation–associated antigen, and thus it does not react with differentiated chondrocytes. iCS cells stained positive for human vimentin, and extracellular matrix was positive for collagen type II, implying that the injected human cells generate cartilage (Figure 4D). Nearly 30% of iCS cells stained positive for Ki-67, indicating that iCS cells continued to replicate in cartilage at 7 wk after injection. iCS cells in the tumor had large nuclei with coarse chromatin structure and one or two nucleoli, and the ratio of nucleus/cytoplasm was large. The tumors generated by iCS cells were histopathologically diagnosed as chondrosarcoma by a certified pathologist (A.U.). Anchorage-independent colony formation is a hallmark of transformation and an in vitro correlate of tumorigenicity in vivo (Cremona and Lloyd, 2009). After cultivation in MethoCult H4034 medium, colony formation was evaluated (Figure 5). The colony-forming assay clearly revealed that iCS cells formed colonies but parental cells did not, indicating that iCS cells are transformed cells with chondrogenic potential.

Generation of chondrocytes from other human somatic cells

In addition to human smooth chorion, we used primary cultured cells from human menstrual blood and placental artery. We obtained 10 and 9 clones, respectively, from menstrual blood–derived cells and placental arterial endothelium. All of them proliferated as a chondrogenic cells with transformation and exhibited the same morphology with iCS in vitro (Figure 6). The growth rates of the clones generated from menstrual blood and placental artery were essentially the same as those of iCS cells. After implantation into the dermal tissue of nude mice, they generated chondrogenic tissue that showed metachromasia with the toluidine blue stain.

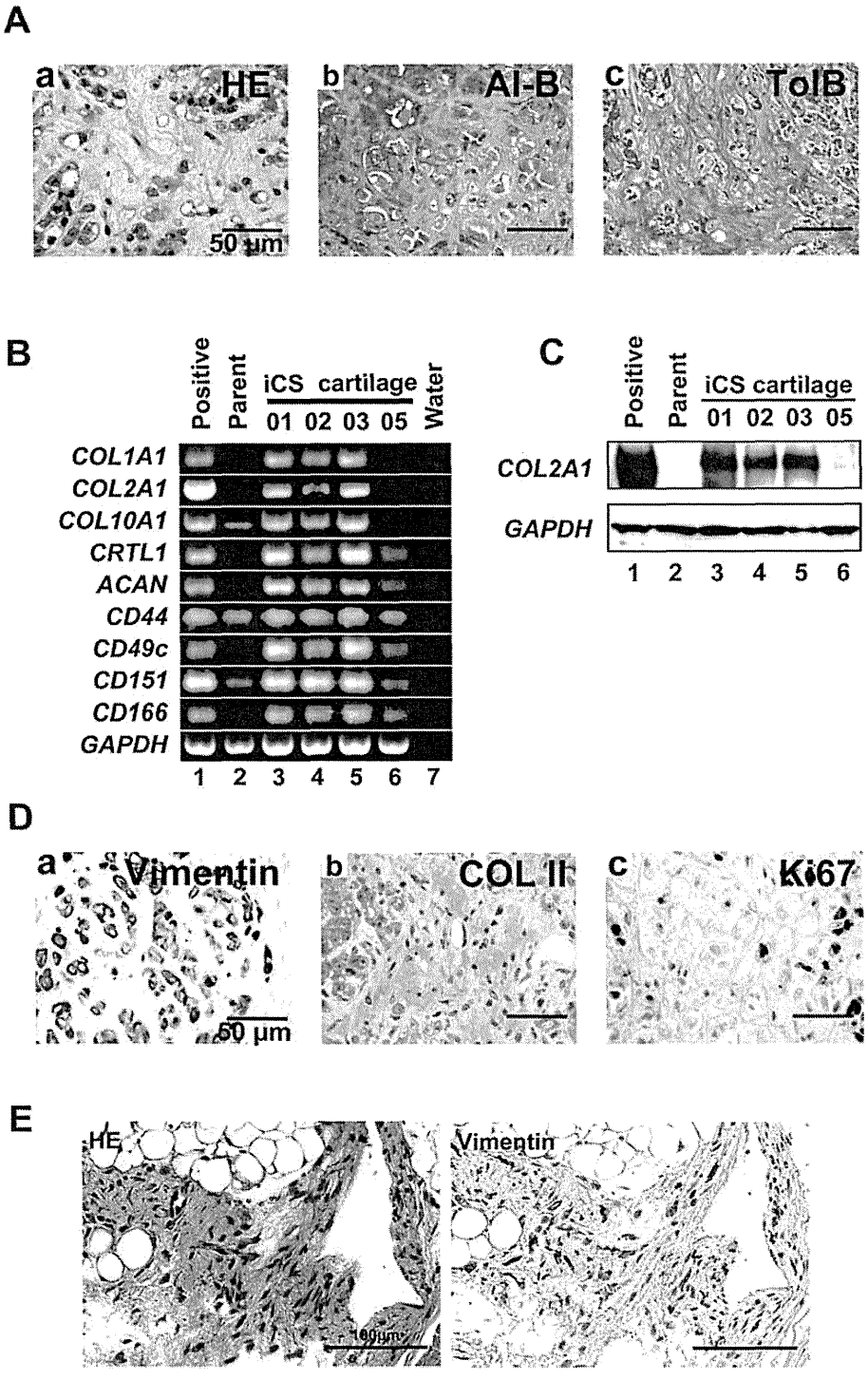

FIGURE 4: In vivo chondrogenic phenotypes of iCS cells. (A) Cartilage at 7 wk after injection of iCS cells. (a) HE stain, (b) Alcian blue, (c) toluidine blue. iCS cells at passage 3 were injected subcutaneously to the dorsal flank of athymic nude mice. Areas of extracellular matrix accumulation stain light to dark blue with Alcian blue (b) or light- to dark-red/purple with toluidine blue (c). Bars, 50 μm. These results are representative of five independent experiments. (B) RT-PCR analysis of the genes encoding SOX5, SOX6, SOX9, COL1A1, COL2A1, COL10A1, CRTL1, and ACAN in cartilage generated by iCS cells. Human cartilage and H_2O (water without RNA) served as positive and negative controls, respectively. Parental cells in culture serve for comparison. (C) Western blot analysis of COL2A1 protein in iCS cartilage at 7 wk after subcutaneous injection of iCS cells into athymic nude mice. Human cartilage serves a positive control. GAPDH was used as a loading control. (D) Immunohistochemical analysis of iCS cartilage. (a) Vimentin, (b) collagen type II (COL II), (c) Ki-67. (E) Implantation of the parental cells. We injected parental cells into athymic nude mice but did not detect any tumor formation. We performed histological analysis and immunohistochemical analysis using the human vimentin-specific antibody. The parental cells did not exhibit cartilage formation at the injected site. Left, HE stain. Right, immunohistochemistry using human-specific antibody to vimentin. Bars, 100 μm.

DISCUSSION

In mammals, cartilage does not regenerate in limb tissue, but cells that derive cartilage retain a strong memory of their embryonic origin in the axolotl (Kragl *et al.*, 2009). Cells are undergoing reprogramming that allows them to reenter embryonic programs of tissue formation, even if they do not revert back to the pluripotent state. Here we show that expression of five transcription factors can rapidly and efficiently convert nonchondrocytes (chorion- and decidua-derived cells) into chondrocytes. iCS cells displayed functional chondrogenic properties such as the generation of extracellular matrices. The possibility of redirecting cell differentiation by overexpression of genes was suggested by Weintraub with the identification of the *MyoD* "master" gene (Davis *et al.*, 1987). The process was believed to involve reversion to a less differentiated state, a kind of dedifferentiation, before the new cell type is formed. Another process has since been suggested, the concept of direct conversion or direct reprogramming without dedifferentiation. This process is believed to be direct lineage switching rather than lineage switching back to a branch point and out again in a different direction. Direct conversion has been shown in β cells, cardiomyocytes, and neurons. A specific combination of three transcription factors (*Ngn3*, *Pdx1*, and *MafA*) reprograms differentiated pancreatic exocrine cells in adult mice into cells that closely resemble β cells (Zhou *et al.*, 2008); a combination of three factors (*Gata4*, *Tbx5*, and *Baf60c*) induces noncardiac mesoderm to differentiate directly into contractile cardiomyocytes (Ieda *et al.*, 2010); and a combination of three factors (*Ascl1*, *Brn2*, and *Myt1l*) converts mouse fibroblasts into functional neurons (Vierbuchen *et al.*, 2010). In this study, we used the strategy of direct conversion to generate chondrocytes from human extraembryonic somatic cells. Based on the same method, murine chondrocytes were generated from skin fibroblasts (Hiramatsu *et al.*, 2011) using the three transcription factors *Sox9*, *c-Myc*, and *Klf4*. *Sox9* is a determinant of chondrogenic lineage (Lefebvre *et al.*, 1997), *c-Myc* is a cell cycle driver (Schmidt, 1999), and *Klf4* is involved in the down-regulation of *p53* (Rowland

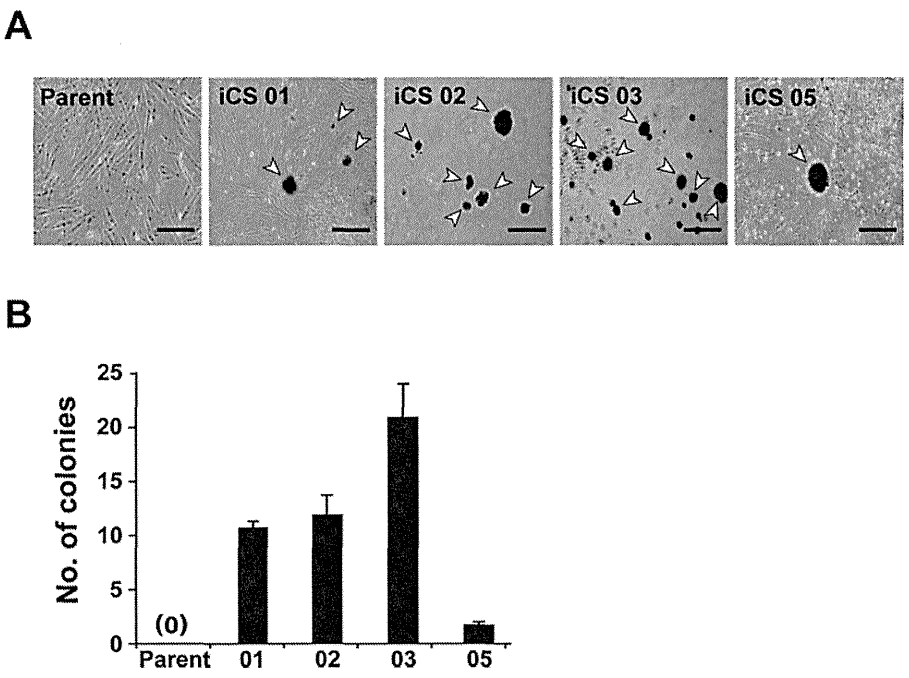

FIGURE 5: Colony formation of iCS cells. (A) Phase contrast micrograph of iCS colonies. iCS cells were cultured in methylcellulose medium on six-well plate dishes. Bars, 500 μm. (B) Number of iCS colonies. Error bars, SD ($n = 9$).

et al., 2005). In this study, *T* and *MITF* may act as inducers of chondrogenic fate determinant, and *BAF60C* may act as epigenetic modifier. *Klf4* was unnecessary for conversion from placental cells to chondrocytes, unlike the reprogramming described for iPS cells (Takahashi and Yamanaka, 2006) and chondrocytes (Hiramatsu *et al.*, 2011). *Baf60c* permits binding of *Gata4* to cardiac genes for reprogramming toward cardiomyocytes (Takeuchi and Bruneau, 2009). Likewise, *BAF60C* may initiate expression of chondrogenic gene sets in combination with *T* and *MITF* in iCS cells.

We showed that the transgene set was sufficient for chondrogenesis without exogenous *SOX9* gene. The *T* gene, one of the transcription factors used in this study, is a member of the T-box family of transcription factors (Papaioannou and Silver, 1998), all of which play key roles during early development, mostly in the formation and differentiation of normal mesoderm (Showell *et al.*, 2004). *T* is also transiently induced in vitro in rhesus monkey embryonic stem cells and mouse embryonal carcinoma cells undergoing mesodermal differentiation (Vidricaire *et al.*, 1994; Behr *et al.*, 2005). Both *T* and *Sox9* are downstream of mitogen-activated protein kinase signaling via fibroblast growth factor receptors in chondrogenesis (Hoffmann *et al.*, 2002). Chondrogenic conversion of the human extraembryonic cells was accompanied by induction of the endogenous *Sox9* gene; however, the induced *Sox9* did not complement reduction of chondrogenesis by siRNA to the *T* gene. *MITF* was also shown to be involved in chondrogenic conversion, although involvement of *MITF* in chondrogenesis has not been reported. *MITF* belongs to an evolutionarily ancient family of the bHLH/LZ proteins (Atchley and Fitch, 1997) and is known to regulate a number of genes of importance in differentiation and maintenance of the melanocytic lineage (Tachibana *et al.*, 1996); conversely, loss-of-function mutations in *MITF* produce depigmentation (Newton *et al.*, 2001). Disruption of *MITF* does not affect chondrocytic differentiation during development, and alternative factors may therefore be present in cells of chondrogenic lineage. The chondrogenesis by *T* and *MITF* may not reflect developmental or physiological pathway, but these two factors are requisite for in vitro chondrogenic conversion of nonchondrocytes.

Stability of the chondrogenic phenotype of iCS cells after long-term cultivation is probably due to lack of transgene silencing—in other words, continuity of transgene expression during cultivation and expression of endogenous chondrogenic genes in some cases. Chondrogenic induction is mediated at least in part by reprogramming, because expression of the endogenous *T* gene was initiated by the five factors. It remains unclear whether the process of the conversion is via dedifferentiation into multipotent, oligopotent stem cells or undifferentiated progenitors. Placenta is developmentally distinct from cartilage, and conversion from placenta to chondrocytes is considered lineage switching or transdifferentiation rather than differentiation. In β cells (Zhou *et al.*, 2008) and retinal cells (Osakada *et al.*, 2009), direct reprogramming is achieved with hepatocytes and iris cells, respectively, which are developmentally close to the generated cells. Successful reprogramming with other somatic cells for parental cells (Figure 6) indicates that the conversion is indeed reprogramming. Autoregulatory feedback and feedforward activation of downstream transcriptional regulators reinforces the expression of important cell fate–determining genes and helps to further stabilize the induced transcriptional program. Robust changes in transcriptional activity can be explained by genome-wide adjustments of repressive and active epigenetic features, such as DNA methylation, histone modifications, and changes of chromatin-remodeling complexes that further stabilize the new transcriptional network (Zhou *et al.*, 2008). It is possible that certain subpopulations of cells are "primed" to respond to these factors, depending on their preexisting transcriptional or epigenetic states (Yamanaka, 2009).

Our study opens an avenue to generate human chondrocytes. Even with the presence of retroviral integration, human iCS cells can possibly be used for tissue engineering experiments such as screening of suitable scaffold of cartilage and can be an alternative to murine ATDC5 teratocarcinoma cells, an ideal cell line for development of tissue engineering strategies aimed at cartilage generation. Once the safety issue, that is, cell transformation, is overcome, iCS cells should also be applicable for repair of defective cartilage in regenerative medicine. We should, however, exercise caution because human iCS cells are not identical to human chondrocytes from the viewpoint of global gene expression. Further studies are essential to determine whether a nontransformed counterpart of iCS can replace chondrocytes in medical applications.

MATERIALS AND METHODS

Preparation of tissue and procedure for cell culture

A human placenta was collected after delivery of a male neonate with the approval of the Ethics Committee of the National Research Institute for Child Health and Development, Tokyo, Japan. Signed informed consent was obtained from the donors, and the specimens were irreversibly deidentified. All experiments handling human cells and tissues were performed in line with the Tenets of the Declaration of Helsinki. This study was wholly carried out at the National Research Institute for Child Health and Development, Tokyo, Japan.

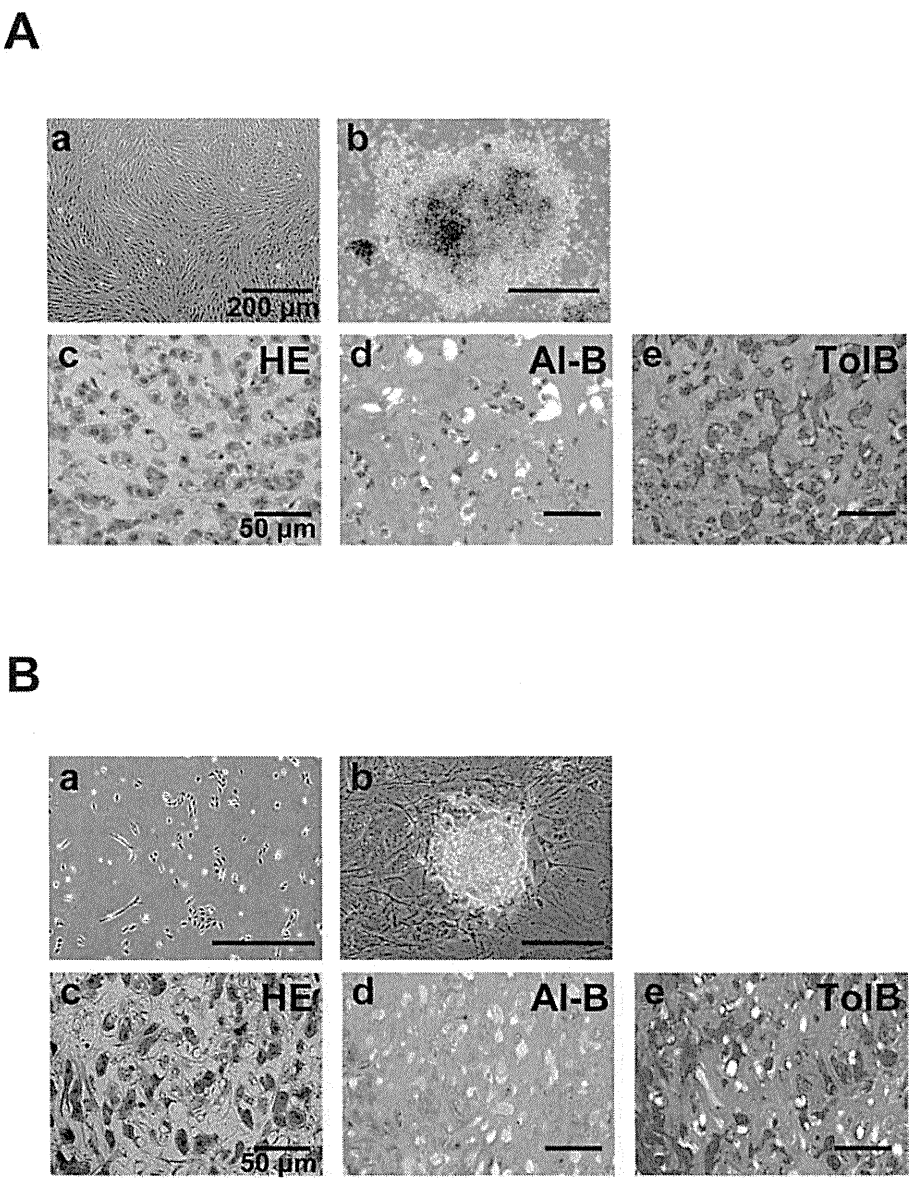

FIGURE 6: Generation of iCS cells from other human somatic cells. (A) iCS generation from human menstrual blood. (a) Phase contrast micrograph of menstrual blood–derived cells. (b) Phase contrast micrograph of iCS cells from menstrual blood. (c–e) Histological analysis of iCS cartilage generated from menstrual blood. (c) HE stain, (d) Alcian blue (Al-B), (e) toluidine blue (TolB). Bars, 200 (a, b) and 50 μm (c–e). (B) iCS generation from human placental artery (hPAE). (a) Phase contrast micrograph of hPAE cells. (b) Phase contrast micrograph of iCS cells from hPAE cells. (c–e) Histological analysis of iCS cartilage generated from hPAE cells. (c) HE stain, (d) Alcian Blue (Al-B), (e) toluidine blue (TolB). Bars, 200 μm (a, b) and 50 μm (c–e).

To isolate placenta-derived cells, we used the explant culture method, in which the cells were outgrown from pieces of chorion and decidual cells attached to dishes (Supplemental Figure S1). Briefly, the smooth chorion and decidua were cut into pieces ~2 mm^3 in size. The pieces were washed in DMEM (high glucose; Sigma-Aldrich, St. Louis, MO) supplemented with 100 U/ml penicillin–streptomycin (Life Technologies, Carlsbad, CA), 1 μg/ml amphotericin B (Life Technologies), and 4 U/ml Novo-Heparin Injection 1000 (Mochida Seiyaku, Tokyo, Japan) until the supernatant was free of erythrocytes. Some pieces were attached to the substratum in a 10-cm dish. The cells migrated out from the cut ends after ~20 d of incubation at 37°C in 5% CO_2. The migrated cells were harvested with Dulbecco's phosphate-buffered saline with 0.1% trypsin and 0.25 mM EDTA for 5 min at 37°C and counted. The harvested cells were reseeded at a density of 3×10^5 cells in a 10-cm dish. Confluent monolayers of cells were subcultured at a 1:8 split ratio onto new 10-cm dishes. The culture medium was replaced with fresh culture medium every 3 or 4 d.

Plasmid construction

Full-length of transcription factors *BCL6*, *T*, *c-MYC*, *MITF*, and *BAF60C* were amplified from cDNAs prepared from total RNA of adult human heart cells (Clontech, Mountain View, CA) and embryonic body-formed iPS cells (day 3–4) by reverse transcription-PCR with the primers listed in Supplementary Table 1, and by digestion with *Hin*dIII sites of pMXs and T4 DNA polymerase accessory they were used for DNA synthesis. The cDNA plasmid was subcloned into pMXs vector using *Hin*dIII restriction sites. pMXs was a gift from T. Kitamura (Tokyo University, Tokyo, Japan).

Retroviral infection

293FT cells (5×10^6) were plated in a 10-cm dish and incubated overnight. The next day, the cells were cotransfected with pMXs-*BCL6*, pMXs-*T*, pMXs-*c-MYC*, pMXs-*MITF*, pMXs- *BAF60C*, pCL-GagPol, and pHCMV-VSV-G vectors with TransIT-293 reagent (Mirus, Madison, WI). The medium was replaced with fresh medium 24 h after transfection. The medium was collected after 48 h as the virus-containing supernatant. Placenta-derived cells in primary culture were seeded at 1×10^5 cells per six-well plate 1 d before infection. The virus-containing supernatants were filtered through a 0.45-μm pore-size filter, ultracentrifuged at 8000 × *g* for 24 h, and then resuspended in Knockout-DMEM (Invitrogen) supplemented with 2 mg/ml Polybrene (Nacalai Tesque, Kyoto, Japan). Cells in six-well plates were transfected with siRNA to the *p53* gene (si*TP53*) using RNAiMAX (Invitrogen, Carlsbad, CA) according to the protocols recommended by the manufacturer (Hong *et al.*, 2009). Cells were transfected overnight, washed, and resuspended in Opti-MEM (Life Technologies/Invitrogen) and were used for virus infection. Cells were trypsinized and plated in six-well plates at 1×10^5 cells per well for 24 h before transfection. Retrovirus cocktail was transferred to cells and incubated for 24 h. After infection, cells were cultured for 5 d and replaced on an irradiated MEF feeder layer in six-well plates. The medium was changed every 2 d with fresh Poweredby10 (GP Biosciences, Yokohama, Japan). Colonies were picked up and transferred into 2-ml Poweredby10 medium at ~10 d after infection. The colonies were mechanically dissociated to small clumps by pipetting up and down. The cell suspension was transferred on irradiated MEF feeder in 60-mm dish (Iwaki; Asahi Techno Glass, Tokyo, Japan). We defined this stage as passage 1.

RT-PCR

Total cellular RNA was isolated from cells using an Isogen extraction kit (Nippon Gene, Tokyo, Japan) according to the manufacturer's protocol. Total RNA (1.0 μg each) for RT-PCR was converted to cDNA with Superscript III RNase H– reverse transcriptase (Invitrogen), according to the manufacturer's manual. PCR conditions were optimized, and the linear amplification range was determined for each primer by varying annealing temperature and cycle number. PCR products were identified by positive control size. Primer sequences are provided in Supplemental Table S1 and Supplemental Figure S5. RT-PCR was performed by using the primers for the genes *BCL6*, *T*, *c-MYC*, *MITF*, *BAF60C*, *COL1A1*, *COL2A1*, *COL10A1*, *CRTL1*, *ACAN*, *SOX5*, *SOX6*, *SOX9*, *TERT*, and *GAPDH*. Adult chondrocyte RNA (Cell Applications (San Diego, CA), human heart RNA (Clontech), and human iPS cell RNA were used as positive controls for RT-PCR analysis. PCR was performed with KOD FX DNA polymerase and PCR buffer (Toyobo, Osaka, Japan), 35 cycles, with each cycle consisting of 95°C for 30 s, 60°C for 45 s, and 72°C for 45 s, with additional 5-min incubation at 72°C after completion of the final cycle. The PCR products were size fractionated by 2% agarose gel electrophoresis.

Quantitative RT-PCR

RNA was extracted from cells using an Isogen extraction kit according to the manufacturer's protocol. An aliquot of total RNA was reverse transcribed by using an oligo(dT) primer. For the thermal cycle reaction, the cDNA template was amplified (PRISM 7900HT Sequence Detection System; Applied Biosystems, Foster City, CA) using the Platinum Quantitative PCR SuperMix-UDG with ROX (11743-100; Invitrogen) under the following reaction conditions: 40 cycles of PCR (95°C for 15 s, and 60°C for 1 min) after an initial denaturation (95°C for 2 min). Fluorescence was monitored during every PCR cycle at the annealing step. The authenticity and size of the PCR products were confirmed using a melting curve analysis (using software provided by Applied Biosystems) and gel analysis. mRNA levels were normalized using *GAPDH* as a housekeeping gene.

Flow cytometric analysis

Cells were stained for 1 h at 4°C with primary antibodies and immunofluorescent secondary antibodies. The cells were then analyzed on a Cytomics FC 500 (Beckman Coulter, Brea, CA), and the data were analyzed with FlowJo, version 7 (Tree Star, Ashland, OR). Antibodies against human CD44, CD49c, CD151, and CD166 (all from BD Biosciences PharMingen, San Diego, CA) were adopted as primary antibodies.

Histological analysis

Infected cells were harvested by trypsin/EDTA treatment, collected into tubes, and centrifuged at 300 × *g* for 5 min, and the pellets were suspended in the DMEM medium. The same volume of Basement Membrane Matrix (BD Biosciences PharMingen) was added to the cell suspension. The cells were implanted subcutaneously to a BALB/c-nu/nu mouse (CREA, Tokyo, Japan) for 7 wk. Tumors were dissected and fixed with phosphate-buffered saline containing 4% paraformaldehyde. Paraffin-embedded tissue was sliced and stained with hematoxylin and eosin.

Western blotting

Semiconfluent cells were lysed with CelLytic M cell Lysis Reagent (Sigma-Aldrich) supplemented with a protease inhibitor cocktail (Sigma-Aldrich). Cell lysates (20 μg each) were separated by electrophoresis on NuPAGE Novex Tris-Acetate gel (Invitrogen), and transferred to Immobilon-P transfer membrane (Millipore, Billerica, MA). The membrane was soaked in protein blocking solution (Blocking One solution; Nacalai Tesque) for 30 min at room temperature before an overnight incubation at 4°C with primary antibody for COL2A1 (1:1000; Santa Cruz Biotechnology, Santa Cruz, CA) and GAPDH (1:1000; Cell Signaling, Beverly, MA) also diluted in blocking solution. The membrane was then washed three times with TBST (20 mM Tris-HCl, pH 7.6, 136 mM NaCl, and 0.1% Tween-20), incubated with a horseradish peroxidase–conjugated secondary antibody (0.04 μg/ml) directed against the primary antibody for 45 min, and washed three times with TBST. The signal was detected by an enhanced ECL Plus Western Blotting Detection System (GE Healthcare, Piscataway, NJ) and an LAS3000 imaging system (Fujifilm, Tokyo, Japan), following the manufacturers' recommendations.

siRNA transfection

The infected cells in six-well plates were transfected with siRNA using Lipofectamine RNAiMAX Reagent (Invitrogen) according to the protocols recommended by the manufacturer (Cui *et al.*, 2011). The cells were harvested 48 h after transfection and analyzed by real-time PCR and RT-PCR.

Gene expression microarray

Total RNA was prepared from duplicate biological samples, and human adult chondrocyte RNA was purchased from Cell Applications. With the use of Low RNA Input Fluorescent Linear Amplification Kits (Agilent Technologies, Santa Clara, CA), cDNA was reverse transcribed from each RNA sample, as well as from a pooled reference control, and cRNA was then transcribed and fluorescently labeled with Cy3. cRNA was purified using an Agilent One Color Spike Mix Kit (Agilent Technologies). We hybridized 1650 ng of Cy3-labeled and amplified cRNA to Agilent 4 × 44 K whole human genome microarrays and processed it according to the manufacturer's instructions. The array was scanned using a G2505B DNA microarray scanner (Agilent Technologies). The image files were extracted using Feature Extraction software, version 10.7.3.1 (Agilent Technologies), with background subtraction and dye normalization. The data were analyzed using GeneSpring GX 10.0 (Agilent Technologies).

Hierarchical clustering analysis and principal component analysis

To analyze the microarray data, we used agglomerative hierarchical clustering and PCA. The hierarchical clustering techniques classify data by similarity using NIA Array Analysis (http://lgsun.grc.nia.nih.gov/ANOVA), and their results are represented by dendrograms. PCA is a multivariate analysis technique that finds major patterns in data variability using TIGR MeV (www.tm4.org/mev.html; Toyoda *et al.*, 2011).

Southern blot analysis

For Southern blot analysis, genomic DNA was isolated using the DNeasy kit (Qiagen, Valencia, CA) according to the manufacturer's protocol, digested with *Spe*I and *Bam*HI for *BCL6*, *Spe*I and *Nco*I for *BAF60C*, *Spe*I and *Bgl*II for *MITF* and *T*, and *Spe*I and *Mfe*I or *Bam*HI and *Mfe*I for *c-MYC*, and separated via 0.8% agarose gel electrophoresis. Transfer was to Hybond-N membranes (GE Healthcare). The membrane was fixed under UV irradiation. The probe was hybridized to the blot and detected using CDP-Star detection reagent (GE Healthcare). Signals from the labeled DNA were quantified using a Hyper film ECL (GE Healthcare).

Short-tandem repeat analysis

Genomic DNA was isolated from cultured cell samples using DNeasy columns (Qiagen). This was used as template for STR analysis using

the PowerPlex 16 System (Promega, Madison, WI) and PRISM instrumentation (Applied Biosystems). Numbers shown denote base pair lengths of the 15 autosomal fragments. The analysis was carried out at Nihon Gene Research Laboratories (Sendai, Japan).

Karyotypic analysis

The cells were fixed with methanol:glacial acetic acid (2:5) three times and dropped onto glass slides (Nihon Gene Research Laboratories). Chromosome spreads were Giemsa banded and photographed. A minimum of 10 metaphase spreads were analyzed for each sample, and they were karyotyped using a chromosome imaging analyzer system (Applied Spectral Imaging, Carlsbad, CA).

Colony formation assay

A total of 50,000 cells were resuspended in MethoCult H4034 medium and plated into a six-well plate. Colonies were counted 14 d after plating.

Gene Expression Omnibus accession numbers

National Center for Biotechnology Information Gene Expression Omnibus gene expression microarray data were submitted under accession number GSE29745.

ACKNOWLEDGMENTS

We express our sincere thanks to M. Yamada for fruitful discussion and critical reading of the manuscript, C. Ketcham for reviewing the manuscript, H. Abe for providing expert technical assistance, and Y. Kajiyama, Y. Suehiro, and K. Saito for secretarial work. This research was supported by grants from the Ministry of Education, Culture, Sports, Science, and Technology of Japan; Ministry of Health, Labor and Welfare Sciences research grants; a Research Grant on Health Science focusing on Drug Innovation from the Japan Health Science Foundation; the Advanced Research for Medical Products Mining Programme of the National Institute of Biomedical Innovation (NIBIO); and a grant from the National Center for Child Health and Development.

REFERENCES

Atchley WR, Fitch WM (1997). A natural classification of the basic helix-loop-helix class of transcription factors. Proc Natl Acad Sci USA 94, 5172–5176.

Behr R, Heneweer C, Viebahn C, Denker HW, Thie M (2005). Epithelial-mesenchymal transition in colonies of rhesus monkey embryonic stem cells: a model for processes involved in gastrulation. Stem Cells 23, 805–816.

Cremona CA, Lloyd AC (2009). Loss of anchorage in checkpoint-deficient cells increases genomic instability and promotes oncogenic transformation. J Cell Sci 122, 3272–3281.

Cui CH, Miyoshi S, Tsuji H, Makino H, Kanzaki S, Kami D, Terai M, Suzuki H, Umezawa A (2011). Dystrophin conferral using human endothelium expressing HLA-E in the non-immunosuppressive murine model of Duchenne muscular dystrophy. Hum Mol Genet 20, 235–244.

Davis RL, Weintraub H, Lassar AB (1987). Expression of a single transfected cDNA converts fibroblasts to myoblasts. Cell 51, 987–1000.

Grogan SP *et al.* (2007). Identification of markers to characterize and sort human articular chondrocytes with enhanced in vitro chondrogenic capacity. Arthritis Rheum 56, 586–595.

Hiramatsu K, Sasagawa S, Outani H, Nakagawa K, Yoshikawa H, Tsumaki N (2011). Generation of hyaline cartilaginous tissue from mouse adult dermal fibroblast culture by defined factors. J Clin Invest 121, 640–657.

Hjorten R *et al.* (2007). Type XXVII collagen at the transition of cartilage to bone during skeletogenesis. Bone 41, 535–542.

Hochedlinger K, Jaenisch R (2006). Nuclear reprogramming and pluripotency. Nature 441, 1061–1067.

Hoffmann A *et al.* (2002). The T-box transcription factor Brachyury mediates cartilage development in mesenchymal stem cell line C3H10T1/2. J Cell Sci 115, 769–781.

Hong H, Takahashi K, Ichisaka T, Aoi T, Kanagawa O, Nakagawa M, Okita K, Yamanaka S (2009). Suppression of induced pluripotent stem cell generation by the p53-p21 pathway. Nature 460, 1132–1135.

Ieda M, Fu JD, Delgado-Olguin P, Vedantham V, Hayashi Y, Bruneau BG, Srivastava D (2010). Direct reprogramming of fibroblasts into functional cardiomyocytes by defined factors. Cell 142, 375–386.

Kragl M, Knapp D, Nacu E, Khattak S, Maden M, Epperlein HH, Tanaka EM (2009). Cells keep a memory of their tissue origin during axolotl limb regeneration. Nature 460, 60–65.

Lefebvre V, Huang W, Harley VR, Goodfellow PN, de Crombrugghe B (1997). SOX9 is a potent activator of the chondrocyte-specific enhancer of the pro alpha1(II) collagen gene. Mol Cell Biol 17, 2336–2346.

Levy C, Fisher DE (2011). Dual roles of lineage restricted transcription factors: the case of MITF in melanocytes. Transcription 2, 19–22.

Newton JM, Cohen-Barak O, Hagiwara N, Gardner JM, Davisson MT, King RA, Brilliant MH (2001). Mutations in the human orthologue of the mouse underwhite gene (uw) underlie a new form of oculocutaneous albinism, OCA4. Am J Hum Genet 69, 981–988.

Orkin SH, Zon LI (2008). Hematopoiesis: an evolving paradigm for stem cell biology. Cell 132, 631–644.

Osakada F, Jin ZB, Hirami Y, Ikeda H, Danjyo T, Watanabe K, Sasai Y, Takahashi M (2009). In vitro differentiation of retinal cells from human pluripotent stem cells by small-molecule induction. J Cell Sci 122, 3169–3179.

Papaioannou VE, Silver LM (1998). The T-box gene family. Bioessays 20, 9–19.

Plaas AH, Wong-Palms S (1993). Biosynthetic mechanisms for the addition of polylactosamine to chondrocyte fibromodulin. J Biol Chem 268, 26634–26644.

Rowland BD, Bernards R, Peeper DS (2005). The KLF4 tumour suppressor is a transcriptional repressor of p53 that acts as a context-dependent oncogene. Nat Cell Biol 7, 1074–1082.

Schmidt EV (1999). The role of c-myc in cellular growth control. Oncogene 18, 2988–2996.

Sekiya I, Vuoristo JT, Larson BL, Prockop DJ (2002). In vitro cartilage formation by human adult stem cells from bone marrow stroma defines the sequence of cellular and molecular events during chondrogenesis. Proc Natl Acad Sci USA 99, 4397–4402.

Shirasawa S, Sekiya I, Sakaguchi Y, Yagishita K, Ichinose S, Muneta T (2006). In vitro chondrogenesis of human synovium-derived mesenchymal stem cells: optimal condition and comparison with bone marrow-derived cells. J Cell Biochem 97, 84–97.

Showell C, Binder O, Conlon FL (2004). T-box genes in early embryogenesis. Dev Dyn 229, 201–218.

Surmann-Schmitt C *et al.* (2009). Wif-1 is expressed at cartilage-mesenchyme interfaces and impedes Wnt3a-mediated inhibition of chondrogenesis. J Cell Sci 122, 3627–3637.

Tachibana M, Takeda K, Nobukuni Y, Urabe K, Long JE, Meyers KA, Aaronson SA, Miki T (1996). Ectopic expression of MITF, a gene for Waardenburg syndrome type 2, converts fibroblasts to cells with melanocyte characteristics. Nat Genet 14, 50–54.

Takahashi K, Yamanaka S (2006). Induction of pluripotent stem cells from mouse embryonic and adult fibroblast cultures by defined factors. Cell 126, 663–676.

Takeuchi JK, Bruneau BG (2009). Directed transdifferentiation of mouse mesoderm to heart tissue by defined factors. Nature 459, 708–711.

Toyoda M *et al.* (2011). Lectin microarray analysis of pluripotent and multipotent stem cells. Genes Cells 16, 1–11.

Vidricaire G, Jardine K, McBurney MW (1994). Expression of the Brachyury gene during mesoderm development in differentiating embryonal carcinoma cell cultures. Development 120, 115–122.

Vierbuchen T, Ostermeier A, Pang ZP, Kokubu Y, Sudhof TC, Wernig M (2010). Direct conversion of fibroblasts to functional neurons by defined factors. Nature 463, 1035–1041.

Yagami K, Suh JY, Enomoto-Iwamoto M, Koyama E, Abrams WR, Shapiro IM, Pacifici M, Iwamoto M (1999). Matrix GLA protein is a developmental regulator of chondrocyte mineralization and, when constitutively expressed, blocks endochondral and intramembranous ossification in the limb. J Cell Biol 147, 1097–1108.

Yamanaka S (2009). Elite and stochastic models for induced pluripotent stem cell generation. Nature 460, 49–52.

Zelzer E, Olsen BR (2003). The genetic basis for skeletal diseases. Nature 423, 343–348.

Zhou Q, Brown J, Kanarek A, Rajagopal J, Melton DA (2008). In vivo reprogramming of adult pancreatic exocrine cells to beta-cells. Nature 455, 627–632.

CHEMICAL REVIEWS

Review

pubs.acs.org/CR

Biomimetic Cell Culture Proteins as Extracellular Matrices for Stem Cell Differentiation

Akon Higuchi,*[,†,‡,§] Qing-Dong Ling,[§,∥] Shih-Tien Hsu,[⊥] and Akihiro Umezawa[‡]

[†]Department of Chemical and Materials Engineering, National Central University, Jhongli, Taoyuan, 32001 Taiwan

[‡]Department of Reproductive Biology, National Research Institute for Child Health and Development, 2-10-1 Okura, Setagaya-ku, Tokyo 157-8535, Japan

[§]Cathay Medical Research Institute, Cathay General Hospital, No. 32, Ln 160, Jian-Cheng Road, Hsi-Chi City, Taipei, 221 Taiwan

[∥]Institute of Systems Biology and Bioinformatics, National Central University, No. 300, Jhongda RD., Jhongli, Taoyuan, 32001 Taiwan

[⊥]Taiwan Landseed Hospital, 77 Kuangtai Road, Pingjen City, Tao-Yuan County, 32405 Taiwan

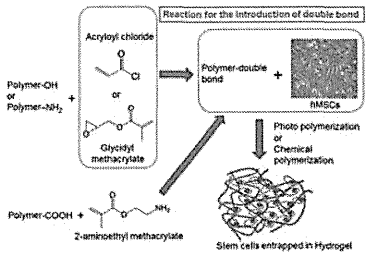

CONTENTS

1. INTRODUCTION

Each year, millions of people suffer loss or damage to organs and tissues due to accidents, birth defects, and disease. Stem cells are an attractive prospect for tissue engineering and regenerative medicine because of their unique biological properties. Embryonic stem cells (ESCs) derived from

Received: January 14, 2012
Published: May 23, 2012

   dx.doi.org/10.1021/cr3000169 | Chem. Rev. 2012, 112, 4507–4540

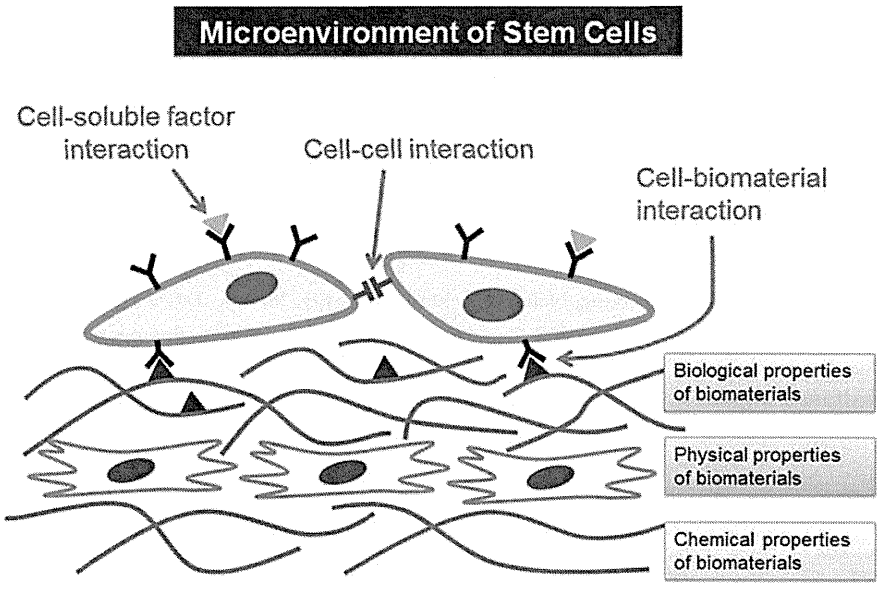

Figure 1. Schematic representation of the microenvironment and niches of stem cells and their regulation by the following factors: (a) soluble factors, such as growth factors or cytokines, nutrients, and bioactive molecules; (b) cell–cell interactions; (c) cell–biomaterial interactions. Biological, physical, and chemical properties of biomaterials also regulate stem cell fate.

preimplantation embryos have the potential to differentiate into any cell type derived from the three germ layers—the ectoderm (epidermal tissues and nerves), mesoderm (muscle, bone, and blood), and endoderm (liver, pancreas, gastrointestinal tract, and lungs).[1] The basis of pluripotency lies in conserved regulatory networks composed of numerous transcription factors and multiple signaling cascades. Together, these regulatory networks maintain human ESCs (hESCs) in a pluripotent and undifferentiated state, and alterations in the stoichiometry of these signals promote differentiation. hESCs have been shown to generate multipotent stem and progenitor cells in vitro and are capable of differentiating into a limited number of cell fates, and thus they have great potential for use in transplantation of cells and tissues into patients.[2]

Although hESCs are promising donor sources for cell transplantation therapies,[1] they face immune rejection after transplantation. Furthermore, ethical issues regarding human embryos hinder their widespread usage. These concerns can be circumvented if pluripotent stem cells can be derived directly from patients' own somatic cells.[3] Recently, pluripotent stem cells similar to ESCs, known as induced pluripotent stem cells (iPSC's), were derived from adult somatic cells by inducing a "forced" expression of certain pluripotent (stem cell) genes[4−6] such as Oct3/4, Sox2, (c-myc), and klf-4, or certain miRNAs[7] or proteins (piPS).[8] iPSC's are believed to be similar to ESCs in many respects, including the expression of certain stem cell genes and proteins, chromatin methylation patterns, doubling time, embryoid body formation, teratoma formation, viable chimera formation, pluripotency, and differentiability.

The pluripotent nature of iPSC's opens many avenues for potential stem cell-based regenerative therapies and for development of drug-discovery platforms.[9,10] The nearest-term therapeutic uses of iPSC's may exist in the transplantation of differentiated nerve cells or β-cells for treatment of Parkinson's Disease and diabetes, respectively, which arise from disorders of single cell types. However, there are several barriers to the clinical application of iPSC's, such as the use of viral vectors, cultivation using xeno-derived materials [e.g., mouse embryonic fibroblasts (MEFs)], and the extremely low efficiency of iPSC generation.[11]

Stem cells have also been isolated from a variety of somatic tissues, including hematopoietic stem cells (HSCs) derived from umbilical cord blood and mesenchymal stem cells (MSCs) derived from bone marrow, umbilical cord blood, umbilical cord, dental pulp, and tissues such as fat. There have been no reports to date of MSCs or fetal stem cells differentiating into tumors, unlike ESCs and iPSC's. Consequently, HSCs, MSCs, and fetal stem cells are the most promising sources of cells for tissue engineering and cell therapies. Currently, MSCs are thought to be the most widely available autologous source of stem cells for practical and clinical applications. Fetal stem cells derived from amniotic fluid are pluripotent cells capable of differentiating into multiple lineages, including cell types of the three embryonic germ layers. Bone marrow MSCs, adipose-derived stem cells (ADSCs), and amniotic fluid stem cells may be more suitable sources of stem cells in regenerative medicine and tissue engineering than ESCs and iPSC's because of ethical concerns regarding their use and concerns about xenogenic contamination arising from the use of mouse embryonic fibroblasts (MEFs) as a feeder layer for ESC and iPSC culture.[11]

Stem cell characteristics, such as proper differentiation and maintenance of pluripotency, are regulated not only by the stem cells themselves but also by the microenvironment. Therefore, mimicking stem cell microenvironments and niches using biopolymers will facilitate the production of large numbers of stem cells and specifically differentiated cells needed for in vitro regenerative medicine. Several factors in the microenvironment and niches of stem cells influence their fate: (i) soluble factors, such as growth factors or cytokines, nutrients, and bioactive molecules; (ii) cell–cell interactions; (iii) cell–biomacromolecule (or biomaterial) interactions; and (iv) physical factors, such as the rigidity of the environment (Figure 1). Some excellent review articles addressing the

engineering of stem cell microenvironments and niches using natural and synthetic biopolymers are listed in Table 1.[11−22]

Table 1. Key Review and Articles Dealing with Biopolymers for Culture and Differentiation of Stem and Progenitor Cells

author	contents	ref (year)
Lee and Mooney	hydrogels for tissue engineering	12 (2001)
Little et al.	biomaterials for neural stem cell microenvironments	13 (2008)
Higuchi et al.	polymeric materials for ex vivo expansion of HSCs	16 (2009)
Mei et al.	combinatorial development of biomaterials for clonal growth of human pluripotent stem cells	17 (2010)
Melkoumian et al.	synthetic peptide-acrylate surfaces for long-term self-renewal of hESCs	18 (2010)
G. J. Delcroix et al.	adult cell therapy for brain neuronal damages and the role of tissue engineering	22 (2010)
Higuchi et al.	biomaterials for the feeder-free culture of hESCs and human iPSC's	11 (2011)
Balakrishnam and Banerjee	biopolymer-based hydrogels for cartilage tissue engineering	14 (2011)
Kim et al.	design of artificial extracellular matrices for tissue engineering	15 (2011)
Engler et al.	matrix elasticity directs stem cell lineage	19 (2006)
Gilbert et al.	substrate elasticity regulates skeletal muscle stem cell self-renewal	20 (2010)
Huebsch et al.	harnessing traction-mediated manipulation of the cell/matrix interface to control stem-cell fate	21 (2010)

These articles focus on biopolymers employed for maintenance of pluripotency of hESCs, iPSC's, or hematopoietic stem cells (HSCs),[16−18] and for specific differentiation lineages such as chondrocytes (cartilage), muscle cells, and neural cells.[13,14,20] There have been no review articles specifically describing extracellular matrix (ECM) scaffolds (ECM in 3D) or ECM-immobilized dish coatings (ECM in 2D) that guide stem cell fates and differentiation. Therefore, this review focuses on the chemical, physical, and biological characteristics of natural biopolymers, especially ECM proteins, which are the major functional biopolymers, and deals with the ability of these biopolymers to guide differentiation of MSCs into osteogenic, chondrogenic, adipogenic, cardiomyogenic, and neural cell lineages.

2. CELL SOURCES AND ANALYSIS OF DIFFERENTIATION LINEAGES OF MSCS

2.1. Cell Sources

Human MSCs (hMSCs), including fetal stem cells, are one of the most widely available autologous sources of stem cells for clinical applications. hMSCs can be obtained from bone marrow,[23,24] adipose tissue,[25,26] dental pulp,[27] and urine,[28] among other sources. Fetal stem cells can be obtained from amniotic fluid,[29−31] umbilical cord,[32−34] menstrual blood,[35,36] umbilical cord blood,[25,34,37] and placenta.[38,39] hMSCs derived from bone marrow and fat are primarily used for biomaterials research on stem cell culture and differentiation because bone marrow MSCs and ADSCs are easily accessible and can be obtained in large quantities. Bone marrow MSCs (BMSCs) are now commercially available from several companies. Stem cell research is facilitated with these stem cell sources because it is not necessary to obtain permission from ethics committees of the Institutional Review Board (IRB) for use of commercially available MSCs. Otherwise, informed consent from donors and permission from the IRB must be obtained.

2.2. Analysis of Differentiation Lineages

MSCs are multipotent stem cells that can be differentiated into various mesodermal lineages, including osteoblasts, chondrocytes (cartilages), adipocytes, myocytes, and cardiomyocytes.[19,40,41] MSCs are also reported to be able to differentiate into ectodermal lineages (e.g., neuron, oligodendrocyte, astrocyte, neural stem cells, and dopamine-secreting cells)[22,42−45] and endodermal lineages (hepatocytes and β-cells),[31,46−52] although with lower probability than mesoderm lineages. Table 2 summarizes methods for characterizing specific differentiated cells from MSCs.[11,34,46,48,51−87]

MSCs differentiate into an osteogenic phenotype in vitro when supplements such as ascorbic acid, β-glycerophosphate, dexamethasone, and/or bone morphogenic protein 2 (BMP-2) are added to the culture medium. Figure 2 shows the expression of several genes and proteins, as well as mineral deposition, by MSCs upon osteogenic differentiation. Runt-related transcription factor 2 (Runx2, also known as Cbfa1, Pebp2αA, and AML3) is a master regulator of osteogenic gene expression and osteoblast differentiation, and it is an early marker of osteogenesis.[88−90] Runx2 activity is stimulated by mitogen-activated protein kinase (MAPK) signaling and is negatively regulated by thrombin-like enzyme 2 (TLE2). Alkaline phosphatase (ALP) activity is an early osteogenic marker, and osteopontin and osteocalcin are late osteogenic markers.[88] Mineral deposition is generated in the late stage of osteogenic differentiation and is detected by Alizarin Red staining (calcium deposition) and von Kossa staining (calcium phosphate deposition).[57,60,62]

MSCs commit to a chondrogenic phenotype when supplied with transforming growth factor-β1 (TGF-β1). Chondrogenic differentiation of MSCs is typically determined by immunostaining for specific proteins, such as collagen type II and Sox9, dye labeling of glycosamino glycans, and evaluation of expression of chondrogenic proteins or transcription factors (such as collagen type II and type X, cartilage oligomeric protein, aggrecan, and Sox9) (Table 2).[63,64,67,70,91] Sulfated glycosaminoglycans (sGAG's) are visualized by staining with Alcian blue.[91] Accumulation of sulfated proteoglycans are also visualized by Safranin O staining.[72]

Only a few groups have investigated adipogenic differentiation of MSCs cultured on natural and artificial biomaterials[53,62,70, 74,75,92] because adipose tissue is in less demand in clinical usage than osteoblasts and cartilage cells. Adipogenic differentiation is also analyzed by immunostaining for specific proteins (vimentin), dye staining of oil droplets, and measuring expression of transcription factors or other marker proteins, such as peroxisome proliferator-activated receptorγ [PPARγ] and adipocyte Protein 2 (aP-2).[53,61,62, 74,75,92] aP-2 is a carrier protein for fatty acids that is primarily expressed in adipocytes.[93] Preadipocytes and mature adipocytes contain multiple or single lipids in cell bodies, respectively. Therefore, Oil Red O or Nile red staining of preadipocytes and mature adipocytes is frequently used for the detection of lipids.

Neural differentiation of MSCs is primarily analyzed by observing characteristic morphologies of neurons, astrocytes, oligodendrocytes, and microglia. Neuronal progenitor cells and early-stage neurons are also identified by Sox1, Sox2, and CD133 gene expression and by nestin and β-tubulin-III

dx.doi.org/10.1021/cr3000169 | Chem. Rev. 2012, 112, 4507−4540

Table 2. Characterization of Differentiation of MSCs into Specific Lineages [Osteoblasts and Chondrocyte (Cartilages)]

differentiation lineage	characterization	specification	ref (example)
1. Osteoblast	morphology	spread shape tends to differentiate into osteoblasts, bonelike nodule formation	53−55
	protein level (immunostaining)	**collagen I**, osteocalcin, osteonectin	56, 57
	surface marker analysis and immunostaining	osteopontin, bisphosphonate [2-(2-pyridinyl)ethylidene-BP] (PEBP), alkaline phosphatase (ALP)	34, 58
	enzyme activity	**alkaline phosphatase**	
	gene level	**runt-related transcription factor 2** [Runx2 or core binding protein A-1 (CBFA-1)], **osterix** (OSX), **osteocalcin** (OCN), **osteopontin** (OPN), **bone sialoprotein** (BSP), alkaline phosphatase, integrin-binding sialoprotein (IBSP), bone γ-carboxyglutamate protein (BGLAP)	34, 58−61
	dye staining	**Alizarin Red staining** (calcium)	62
	mineral deposition	**von Kossa staining** (calcium phosphate)	57, 60
2. Chondrocytes	protein level (immunostaining)	**collagen type II** (Col II), **collagen type X** (Col X), **aggrecan** (AGN), Sox-9, chondroitin-4-sulfate, chondroitin-6-sulfate, sulphated glycosaminoglycans	56, 57, 63−68
	glycosaminoglycan assay	glycosaminoglycan content	
	dimethylmethylene blue (DMMB) assay	proteoglycan (PG) content	69
	hydroxyproline assay	collagen content	65
	gene level	**collagen II**, collagen IX (Col IX), **collagen X**, collagen XI (Col XI), **aggrecan**, Sox 5, Sox 6, **Sox 9**, **cartilage oligomeric protein** (COMP), xylosyltransferase I (XT-1), α-4-*N*-acetylhexosaminyltransferase (EXTL2), β-1,4-*N*-acetylgalactosaminyltransferase (GalNAcT), glucuronyl C5 epimerase (GlcAC5E)	63, 64, 67, 70−73
	dye staining	**Safanin O staining (proteoglycan)**, **Alcian blue staining (proteoglycan)**, EVG-staining, Masson's trichrome staining	34, 62, 64, 67, 70, 72
3. Adipocytes	morphology	round shape cells tends to differentiated into adipocytes	53, 54
	protein level	vimentin, adipocyte lipid-binding protein (ALBP)	53, 74
	enzyme activity	glycerol-3-phosphate dehydrogenase activity	75
	gene level	PPARγ, aP-2	61
	staining	Oil red O and Nile red staining for lipid droplet	62
4. Neural cells	morphology	neuronal-like cells having long neurites	76
	protein level	nestin, neuron-specific class III β-tubulin (TuJ1), galactosylceramidase (GalC), glial fibrillary acidic protein (GFAP), β-tubulin-III, microtubule-associated protein 2 (MAP2), O4, tyrosine hydroxylase (TH), neurofibromatosis (NFM), neurone-specific enolase (NSE)	76−81
	gene level	nestin, Musashi 1, neuron-specific class III β-tubulin (TuJ1), glial fibrillary acidic protein, microtubule-associated protein 2, Sox1, Sox2, CD133, tyrosine hydroxylase, neurofibromatosis, Nurr1, dopamine transporter (DAT), dihydropyrimidinase-related protein 2 (DRP-2), purine-sensitive aminopeptidase (PSA)	11, 61, 76, 81, 82
5. Cardiomyocytes	morphology	contractile cells	
	protein level	**cardiac troponin T (cTnT)**, **desmin**, myosin light chain (MLC), myosin heavy chain (MHC)	81
	gene level	Nkx2.5, GATA-4, MYH-6, TNNT2, TBX-5, myosin light chain (Mlc2a, MLC-2 V), tropomyosin, cTnI, ANP, **desmin**, **myosin heavy chain** (α-MHC, **β-MHC**), **cardiac troponin T**, Isl-1, and Mef2c	11
	electrocardiogram	electrocardiogram	
6. Smooth muscle cells	protein level	α-smooth muscle actin (ASMA), h1-calponin (CALP), SM2	83
	gene level	α-smooth muscle actin, h1-calponin, caldesmon, Smemb, SM22α, SM1, SM2	83
7. Epidermis	protein level	keratin 10 (early marker), filaggrin (intermediate marker), involucrin (late marker)	84
	gene level	keratin 10 (early marker), filaggrin (intermediate marker), involucrin (late marker)	84
8. Hepatocyte	morphology	oval cell morphology, small round cell morphology	46

dx.doi.org/10.1021/cr3000169 | *Chem. Rev.* 2012, 112, 4507−4540

Table 2. continued

differentiation lineage	characterization	specification	ref (example)
	protein level	CXCR4 (endoderm), α-fetoprotein (AFP), albumin (ALB), asialoglycoprotein receptor (ASGPR), cytochrome P450 (CYP_1A_1), hepatocyte nuclear factor-1α (HNF-1α), hepatocyte nuclear factor-3β (HNF-3β), hepatocyte nuclear factor-4α (HNF-4α), CCAAT-enhancer binding protein α (C/EBPα), cytokeratin-18 (CK18), cytokeratin-19 (CK19), low-density lipoprotein (LDL), GATA4	46, 51, 52, 86, 87, 113
	gene level	Sox17 (endoderm), Foxa2 (endoderm), Gata6 (endoderm), α-fetoprotein, albumin, hepatocyte nuclear factor-1α, hepatocyte nuclear factor-3β, hepatocyte nuclear factor-4α, cytokeratin 18, cytokeratin-19, asialoglycoprotein receptor, tryptophan oxygenase (TO), cytochrome P450 (CYP1A1, CYP2B6), CCAAT-enhancer binding protein α, glucose 6-phosphate (G6P), GATA4	46, 51, 52, 86, 87, 113
	urea assay	urea production	46, 51, 113
	albumin assay	albumin production	52, 86, 113
	glycogen assay	glycogen production	46, 52, 113
	α-fetoprotein assay	α-fetoprotein production	52, 86
	pentoxyresorufin (PROD) assay	cytochrome P450 activity	113
	staining	periodic acid–Schiff (PAS) staining for glycogen storage	46, 113

immunostaining. Mature neurons express neuron-specific class III β-tubulin (Tuj1), microtubule-associated protein 2 (MAP2), neuron-specific enolase (NSE), and purine-sensitive aminopeptidase (PSA). Oligodendrocytes express galactosylceramidase (GalC) and O4. Dopaminergic neurons express tyrosine hydroxylase (TH), neurofibromatosis (NFM), and dopamine transporter (DAT). Nerve cells are electrically excitable cells that transmit information by electrical and chemical signaling. Therefore, electrical and action potentials in nerve cells can be monitored using electrodes.

3. PREPARATION OF CULTURE MATRIX

Biomimetic stem cell cultures can be categorized as two-dimensional (2D) or three-dimensional (3D). 2D culture is useful for basic research to investigate the fundamental interactions between cells and immobilized nanosegments on dishes, but 3D culture of stem cells in biomaterials is essential for clinical applications. Figure 3 shows some examples of biomaterial designs for carrying stem cells, as well as direct injection of biomaterials without cells. The injection of hydrogels or scaffolds containing stem cells is categorized as 3D cultures. Cell sheets prepared on a surface-grafting polymer having low critical solution temperature (LCST), such as poly(*N*-isopropylacrylamide) (poly(NIPAM)), can be prepared on 2D dishes.[94,95] Recently, patch sheets of immobilized antibodies or ligands targeting specific stem cells, which recruit the stem cells from the patient's body, are reported to be effective in gathering autologous stem cells at sites of injury.[40] The following sections describe methods for (a) surface immobilization of ECM proteins and ECM-mimicking peptides on 2D culture dishes and (b) preparing hydrogels or scaffolds containing ECM proteins and ECM-mimicking peptides for 3D culture of stem cells.

3.1. ECM Immobilization on 2D Dishes

Typically, 2D cell culture dishes are coated with ECM proteins or ECM-mimicking peptides. Tables 3 and 4 show examples of the ECM proteins and ECM-mimicking peptides used to coat culture dishes and their binding sites on stem cells.[16,18,53,58,71,83,91,96–118] Collagen types I, II, and IV, gelatin, laminin, laminin-1, laminin-5, vitronectin, and fibronectin are typically used as coating materials.[58,71,83,91,96–98,100–102] ECM-mimicking peptides (e.g., RGD, DGEA, YIGSR, IKVAV, KRSR, P15, and GFOGER) are commonly used as coating or grafting materials.[16,18,53,97,103–118] Covalent binding is preferable for long-term effects in culture, but noncovalent coating is the simplest method for the preparation of dishes with immobilized ECM proteins or ECM-mimicking peptides. Figure 4 summarizes typical surface reactions for the covalent immobilization of ECM proteins and peptides on dishes. Proteins and ECM-mimicking peptides should be used in aqueous solution, as they are unstable biomolecules. Reactions between amino groups and between amino groups and carboxylic acids can be used to bind ECM proteins and ECM-mimicking peptides to plastic dishes. These plastic surfaces should therefore have amino groups, carboxylic acid groups, or hydroxyl groups to bind and immobilize ECM proteins or peptides. For dishes made of polyesters, such as poly(ε-caprolactone) (PCL), poly(glycolic acid) (PGA), poly(lactic acid) (PLA), or poly(lactic acid-*co*-glycolic acid) (PLGA), treatment with a diamine, such as hexamethylene diamine, generates amino groups on the surface by an aminolysis reaction. Then, ECM proteins and ECM-mimicking

dx.doi.org/10.1021/cr3000169 | Chem. Rev. 2012, 112, 4507–4540

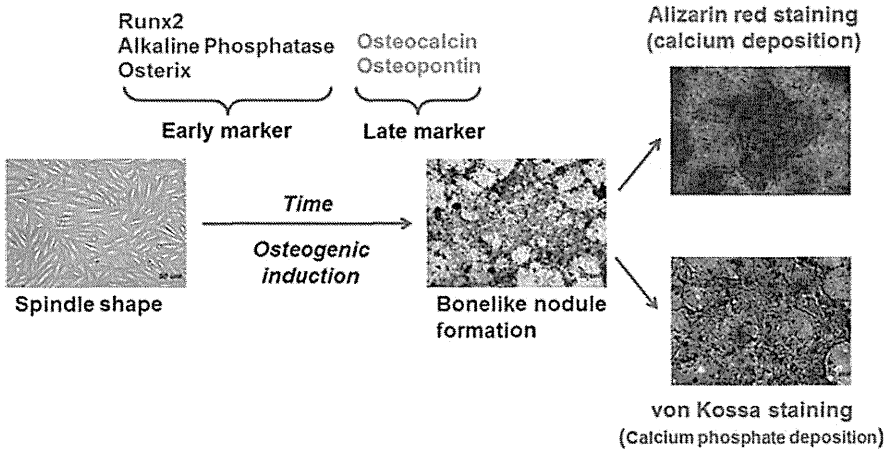

Figure 2. Osteogenic differentiation of MSCs, gene expression, and mineral deposition at early and late stages.

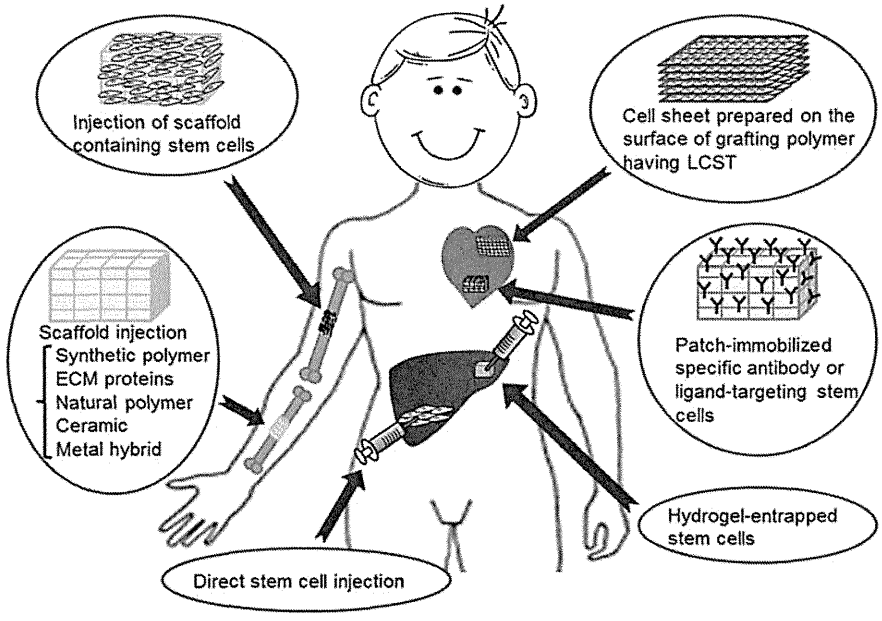

Figure 3. Some examples of biomaterial designs with and without stem cells for the injection of biomaterials in clinical applications: (a) injection of scaffold containing stem cells, (b) injection of scaffold without cells, (c) direct stem cell injection, (d) injection of cell sheets, (e) injection of patch-immobilized specific antibody or ligand-targeting stem cells, and (f) injection of hydrogel-entrapped stem cells.

peptides can be covalently immobilized using hexamethylene diisocyanate (HMDIC), 1,6-dimethyl suberimidate dihydrochloride (DMS),[119] or NHS/EDC reagent,[18] where NHS is *N*-hydroxysuccinimide and EDC is *N*-(3-dimethylaminopropyl)-*N*′-ethylcarbodiimide (Figure 4). EDC is a water-soluble carbodiimide that is generally used in the 4.0–6.0 pH range. Therefore, it is possible to immobilize ECM proteins and ECM-mimicking peptides in aqueous solution using NHS/EDC reagents. The covalent bonding between amino groups can be reacted with aqueous DMS.[119]

Genipin is generally used to cross-link proteins, such as collagen and gelatin, and chitosan via amino groups.[120,121] Genipin can also be used for the immobilization of ECM proteins and peptides on the surface of culture dishes with amino groups (Figure 4). NHS/EDC, DMS, and genipin are the recommended reagents to covalently immobilize ECM proteins and ECM-mimicking peptides on culture dishes.

3.2. 3D Culture in Hydrogels

Hydrogels are physically or chemically cross-linked polymer networks that are able to absorb large amounts of water. Injectable hydrogels containing stem cells can be delivered to sites of damage in patients with minimal invasiveness, and the hydrogels ensure that stem cells remain localized to the damaged sites more effectively than injected cells alone. Physical cross-linking is performed on ECM proteins with thermosensitive properties of lower critical solution temperature (LCST) or upper critical solution temperature (UCST), such as collagen and gelatin. Collagen can be dissolved in aqueous solutions at low temperature and forms gels at ~37 °C because of its LCST characteristics, and gelatin can be dissolved in aqueous solution at high temperatures and forms gels at room temperature because of its UCST. Therefore, stem cells can be dissolved in ECM protein solutions and efficiently entrapped in ECM gels at 20–37 °C. However, most ECM

Table 3. ECM Immobilized on Dishes for Adhesion, Differentiation, And Proliferation of Stem Cells and Some Examples of the Literature

ECM	binding site of cells	ref
collagen I	integrin ($\alpha V\beta 3$, $\alpha 2\beta 1$)	58, 96
collagen I	integrin ($\alpha 1\beta 1$)	97
collagen I	integrin ($\alpha 1\beta 1$, $\alpha 2\beta 1$, $\alpha 3\beta 1$)	71
collagen II	integrin ($\alpha 1\beta 1$, $\alpha 2\beta 1$, $\alpha 10\beta 1$)	71, 91
collagen IV	integrin ($\alpha 2\beta 1$, CD44)	98
gelatin		99
fibronectin	integrin ($\alpha 4\beta 1$, $\alpha 5\beta 1$, $\alpha V\beta 3$, $\alpha IIb\beta 3$, $\alpha V\beta 6$, $\alpha V\beta 5$)	58, 96
laminin	integrin ($\alpha 1\beta 1$, $\alpha 2\beta 1$, $\alpha 3\beta 1$, $\alpha 6\beta 1$, $\alpha 6\beta 4$)	100
laminin-1 (laminin 111)	integrin ($\alpha 1\beta 1$, $\alpha 2\beta 1$, $\alpha 6\beta 1$, $\alpha 7\beta 1$, $\alpha 9\beta 1$), α-dystroglycan, suifade, and heparan sulfate proteoglycan	83, 101
laminin-5 (laminin 332)	integrin ($\alpha 2\beta 1$, $\alpha 3\beta 1$, $\alpha 6\beta 1$, $\alpha 6\beta 4$)	102
laminin-10/11	integrin ($\alpha 3\beta 1$, $\alpha 6\beta 1$, $\alpha 6\beta 4$)	100
vitronectin	integrin ($\alpha V\beta 3$, $\alpha V\beta 5$)	58, 96

proteins and ECM-derived oligopeptides (ECM peptides) need other forms of cross-linking to trap stem cells and generate hydrogels. Typically, photocross-linking and chemical cross-linking of ECM proteins and ECM peptides are used. There are several excellent reviews that discuss hydrogel preparation and reaction in detail.[12,14] Therefore, this section deals briefly with the preparation of ECM hydrogels using photocross-linking and chemical cross-linking with cross-linking agents. The application of ECM hydrogels containing stem cells is discussed in section 5 for specific ECM proteins and ECM peptides.

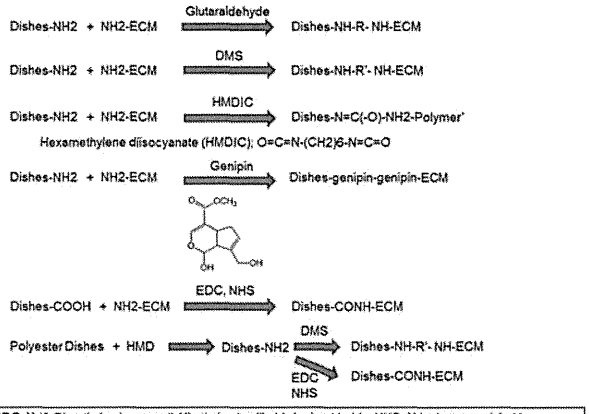

Figure 4. Surface reactions of covalent immobilization of ECM proteins and ECM-mimicking peptides on dishes.

3.2.1. Photocross-Linking of ECM Proteins and ECM Peptides. Hydrogels containing stem cells can be easily prepared by UV irradiation of ECM proteins and ECM–peptide solutions. These preparations can be used as injectable hydrogels via photocross-linking. However, it is first necessary to introduce double bonds into ECM proteins and ECM peptides for photocross-linking. ECM proteins and ECM peptides have $-OH$, $-NH_2$, and $-COOH$ functional groups. Double bonds can be introduced into ECM proteins and ECM

Table 4. ECM-Mimicking Peptides Immobilized on Dishes for Adhesion, Differentiation, And Proliferation of Stem Cells

ECM-mimicking peptide	ECM proteins for mimicking	binding site of cells	ref
DGEA	collagen I	integrin ($\alpha 2\beta 1$)	103–105
GTPGPQGIAGQRGVV (P15)	collagen I	integrin ($\alpha 2\beta 1$)	103, 106
$(RADA)_4$GG**DGEA**	collagen I	integrin ($\alpha 2\beta 1$)	116
$(RADA)_4$GGFPGERGVEGPGP	collagen I		116
GFOGER	collagen	integrin ($\alpha 2\beta 1$)	103, 107, 108
MNYYSNS	collagen IV		109
RGD	collagen I	integrin ($\alpha V\beta 3$)	97, 110
ELIDVPST (CS-1)	fibronectin	integrin ($\alpha 4\beta 1$); VLA-4	16, 111
FN-40	fibronectin	integrin ($\alpha 4\beta 1$, VLA-4)	16, 112
FN-120	fibronectin	integrin ($\alpha 5\beta 1$); VLA-5	16, 112
FN–CH296	fibronectin	integrin ($\alpha 4\beta 1$, $\alpha 5\beta 1$)	16, 112
KGGAVT**GRGDS**PASS	fibronectin	integrin ($\alpha 5\beta 1$); VLA-5	18, 113
GRGDSPK	fibronectin	integrin ($\alpha 5\beta 1$); VLA-5	18, 113
KNNQKSEPLIGRKKT	fibronectin	heparin-binding domain	53
RGDS	fibronectin		109
PHSRN	fibronectin		109
KYGAAS**IKVAV**SADR	laminin		18, 114
YIGSR	laminin		109
IKVAV	laminin		115
PPFLMLLKGSTR	laminin-5 (laminin332)	integrin ($\alpha 3\beta 1$)	
(RADA)4-GG**PDSGR**	laminin		116
(RADA)4-GGSDPG**YIGSR**	laminin		116
(RADA)4-GGIKVAV	laminin		116
KGGPQVT**RGD**VFTMP	vitronectin	integrin ($\alpha V\beta 5$)	18, 117
KGGNGEP**RGD**TYRAY	bone sialoprotein (BSP)		18, 118
PEO4-NGEP**RGD**TYRAY	BSP-linker		18, 118
RGD	osteopontin	integrin ($\alpha V\beta 3$)	97

dx.doi.org/10.1021/cr3000169 | Chem. Rev. 2012, 112, 4507–4540

peptides by the reactions of acryloyl chloride,[122] glycidyl methacrylate,[12,123] and 2-aminoethylmethacrylate[12,124] (Figure 5). Figure 5 also shows a schematic for preparation method of

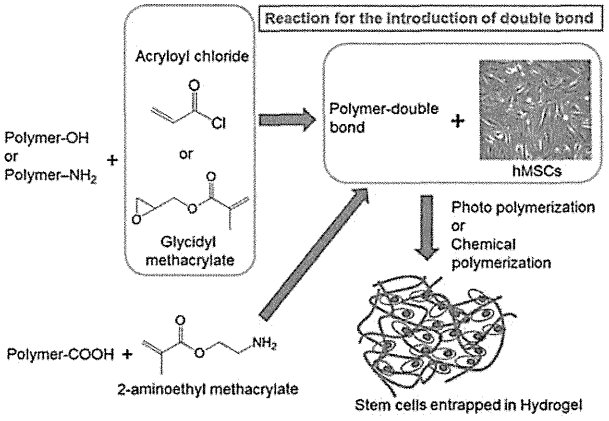

Figure 5. Schematic of the preparation method of hydrogels with entrapped stem cells by photopolymerization.

hydrogels with entrapped stem cells by photopolymerization. Aqueous solutions containing stem cells and macromers of ECM proteins and ECM peptides are irradiated with UV light to generate hydrogels with entrapped stem cells.

Poly(ethylene glycol)diacrylate (PEODA) is typically added to the reaction solution to generate optimal hydrogels.[65,125−129] Yang et al. prepared PEODA hydrogels incorporating RGD adhesive peptides and goat BMSCs by photopolymerization. They found that RGD-conjugated PEODA hydrogels promoted the osteogenic differentiation of BMSCs, and RGD enhanced differentiation in a dosage-dependent manner, with the highest concentration (2.5 mM) in the reaction solution being optimal in their study.[125]

3.2.2. Chemical Cross-Linking of Hydrogels. Hydrogels of ECM proteins can also be prepared by chemical cross-linking. Similar to ECM protein immobilization on 2D dishes, as discussed in section 3.1, NHS/EDC, DMS, HMDIC, and genipin are typically used as cross-linking agents. Glutaraldehyde is not commonly used for the preparation of hydrogels in tissue engineering because it is relatively toxic to stem cells. DMS, HMDIC, and genipin allow cross-linking between amino groups, whereas NHS/EDC leads to cross-linking between carboxylic acids and amino groups in ECM proteins.

Chang et al. compared gelatin hydrogels cross-linked with genipin and gelatin hydrogels cross-linked with glutaraldehyde.[120] They found that the degree of inflammatory reaction in wounds treated with the genipin-cross-linked gelatin was significantly less severe than those covered with the glutaraldehyde-cross-linked gelatin in vivo.[120] In addition, the healing rates of wounds treated with the genipin-cross-linked gelatin were notably faster than those with glutaraldehyde-cross-linked hydrogels.[120]

3.3. 3D Culture in Scaffolds

Scaffolds seeded with stem cells can support 3D tissue formation artificially. It is optimal for scaffolds (a) to allow cell attachment and migration, (b) to allow diffusion of nutrients, growth factors, and waste secreted by cells, and (c) to have mechanical properties similar to the natural tissue. Most of the scaffolds have high porosity (>80%) and large pore size (200−800 μm), which allow diffusion of nutrients, growth factors, and waste, but these properties also lead to weak mechanical properties. Biodegradability of scaffolds is often required because scaffolds should be absorbed by the surrounding tissues without the necessity of surgical removal. It is preferable that the degradation rate of scaffolds should be matched to the speed of tissue formation. The degradation speed of scaffolds can be regulated by the degree of cross-linking. Scaffolds prepared from ECM proteins and ECM peptides are desirable because of their biodegradable characteristics. ECM proteins used for the preparation of scaffolds are typically collagen type I, collagen type II, gelatin, fibronectin, laminin, and vitronectin. ECM proteins can be used as (a) coating materials, (b) blending materials, and (c) main materials of scaffolds.

3.3.1. Preparation of Scaffolds. There are several methods used to prepare scaffolds for tissue engineering and 3D culture of stem cells, including (a) freeze-drying, (b) salt leaching, (c) porogen leaching, (d) use of nonwoven fabric or mesh, (e) nanotopography, and (f) electrospinning. In the freeze-drying method, ECM proteins are dissolved in a buffer solution. The ECM solution is frozen at −20 or −80 °C and then lyophilized in a freeze-dryer before being washed and stored (Figure 6). If necessary, the scaffolds are also cross-linked.

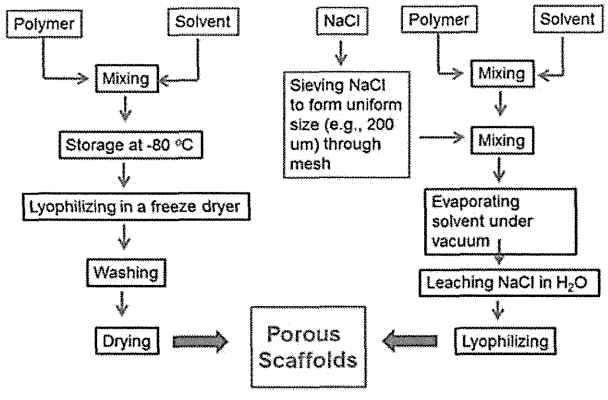

Figure 6. Typical preparation method of porous scaffolds by freeze-drying (a) and salt leaching (b).

The salt-leaching method is as follows. Biopolymers and/or ECM proteins are dissolved in a solvent. Salt, typically NaCl, is sieved to generate a uniform distribution of size using filtration through mesh and added into the solution. The solvent of the solution is vaporized under vacuum to generate dry scaffolds. Salt is then leached from the scaffolds by immersion in water after drying the scaffolds (Figure 6). The porogen-leaching method is a similar method to the salt-leaching method, but other uniformly sized particles, such as polymeric particles, are used instead of salt.

3.4. 3D Culture in Nanofibers

Peptide amphiphiles (PAs), which have a hydrophilic domain and a hydrophobic domain, are known to spontaneously generate self-assembled nanofibers above critical micelle concentrations.[109,116,130] MSC differentiation on self-assembled nanofibers using ECM peptides is discussed in section 5.8.1.

A typical method to create nanofibers is electrospinning. Electrospun scaffolds can support cell adhesion and growth and

dx.doi.org/10.1021/cr3000169 | Chem. Rev. 2012, 112, 4507−4540

promote differentiation of stem cells.[131] Nanofibers can be generated from a spinning nozzle when high voltage is applied between the spinning nozzle and a flat metal collector. Typical electrospinning products are flat and highly interconnected scaffolds with a nonwoven fabric sheetlike morphology. These characteristics hinder cell infiltration and growth throughout the scaffolds. Blakeney et al. have developed a three-dimensional cotton ball-like electrospun scaffold that consists of low-density, uncompressed nanofibers.[131] A grounded spherical dish and an array of needle-like probes were used instead of a traditional flat-plate collector to create a cotton ball-like scaffold. Scanning electron microscopy showed that the cotton ball-like scaffold consisted of electrospun nanofibers with a similar diameter, but with larger pores and less dense structures than traditional electrospun scaffolds.[131] The cotton-ball like scaffolds prepared from ECM proteins by electrospinning will be interesting for use as scaffolds for guiding specific lineages of stem cell differentiation.

4. PHYSICAL PROPERTIES OF BIOPOLYMERS (BIOMATERIALS) GUIDE STEM CELL DIFFERENTIATION FATE (LINEAGE)

The interactions between MSCs and ECM proteins are classified as physical, chemical, and biological. It has recently been recognized that stem cell differentiation is directed by physical properties of culture materials as well as by biochemical responses to growth factors and ECM proteins.[19,20,132] Cells in bone, muscle, liver, and brain tissues reside in different environments that have diverse physical properties.[133] The matrix stiffness for differentiated cells is known to influence focal-adhesion structure and the cytoskeleton.[134−139] Engler et al. reported that soft materials, with similar stiffness to the brain, tend to differentiate MSCs into neurogenic cells, whereas stiffer materials that mimic muscle guide MSCs into myogenic cells and rigid materials similar to collagenous bone induce osteogenic differentiation (Figure 7).[19] However, this work was performed on a 2D surface of hydrogels coated with collagen. The effect of stiffness in 3D culture may produce different results than in 2D culture.

Gilbert et al. also reported that the elasticity of culture materials regulates self-renewal of skeletal muscle stem cells.[20]

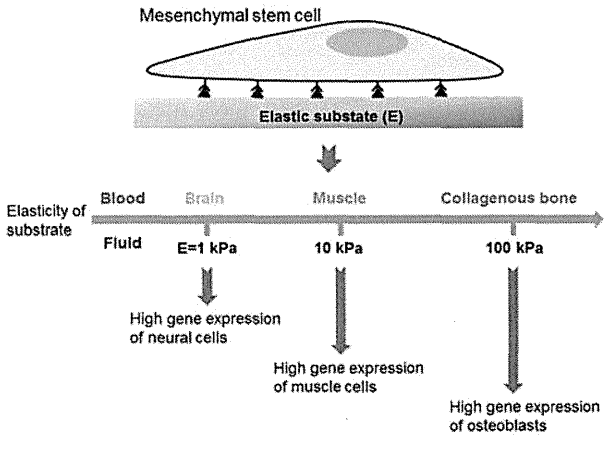

Figure 7. Physical properties decide the fate of stem cell cultured on biomaterials with different elasticity. Modified with permission from ref 19. Copyright 2006 Elsevier Inc.

Muscle stem cells (MuSC's) exhibit robust regenerative capacity in vivo, but this capacity is rapidly lost in culture. They showed that the elasticity of culture materials was a potent regulator of MuSC fate. MuSC's cultured on soft hydrogel substrates that mimicked the elasticity of muscle (12 kPa) self-renew in vitro and contributed extensively to muscle regeneration when transplanted into mice, unlike MuSC's grown on rigid plastic dishes (~106 kPa), as shown by histology and bioluminescence imaging. These studies provide evidence that propagation of adult muscle stem cells is possible by recapitulating physiological tissue rigidity.[20] This finding may contribute to future cell-based therapies for muscle-wasting diseases.

The effect of physical interactions between MSCs and culture materials on stem cell fate is discussed in several articles.[19,20,61,133,140−154] Some landmark findings are summarized in Table 5, and some examples of physical effects on differentiation of MSCs cultured on ECM proteins are reviewed here.

Table 5. Some Articles Discussing Physical Effect of Substrates on Differentiation of MSCs Cultured on the Substrates

authors	contents	ref (year)
J. R. Mauney et al.	**mechanical stimulation** promotes osteogenic differentiation of hBMSCs	140 (2004)
J. S. Park et al.	differential effects of **equiaxial and uniaxial strain** on MSCs	141 (2004)
V. E. Meyers et al.	**microgravity** disrupts collagen I/integrin signaling during osteogenic differentiation of hMSCs	142 (2004)
V. I. Sikavitsas et al.	**flow perfusion** enhances the calcified matrix deposition of marrow stromal cells in scaffolds	143 (2005)
H. Hosseinkhani et al.	**perfusion culture** enhances osteogenic differentiation of MSCs	144 (2005)
A. J. Engler et al.	**matrix elasticity** directs stem cell lineage specification	19 (2006)
R. D. Sumanasinghe et al.	osteogenic differentiation of hMSCs in collagen matrices: effect of **uniaxial cyclic tensile strain**	145 (2006)
D. F. Ward et al.	**mechanical strain** promotes osteogenic differentiation of hMSCs	61 (2007)
E. K. F. Yim et al.	**nanostructures** inducing differentiation of hMSCs into neurinal lihneage	154 (2007)
B. Lanfer et al.	growth and differentiation of MSCs on **aligned collagen** matrices	146 (2009)
Q. Li et al.	ECM with the **rigidity** of adipose tissue helps adipocytes maintain insulin responsiveness	147 (2009)
M. Zscharnack et al.	**low O_2** expansion improves subsequent chondrogenesis of BMSCs in hydrogel	148 (2009)
C. H. Huang et al.	interactive effects of **mechanical stretching** and ECM proteins on initiating osteogenic differentiation of hMSCs	149 (2009)
P. M. Gilbert et al.	substrate **elasticity** regulates skeletal muscle stem cell self-renewal in culture	20 (2010)
G. C. Reilly and A. J. Engler	intrinsic ECM properties regulate stem cell differentiation (**mechanobiology**)	150 (2010)
J. M. Kemppainen and S. J. Hollister	differential effects of **designed scaffold** permeability on chondrogenesis by BMSCs	151 (2010)
E. K. F. Yim et al.	**nanotopography**-induced changes in focal adhesions, cytoskeletal organization, and mechanical properties of hMSCs	152 (2010)
J. Tang et al.	regulation of stem cell differentiation by cell−cell contact on **micropatterned** material surfaces	153 (2010)
P. A. Janmey and R. T. Miller	mechanisms of **mechanical** signaling in development and disease	133 (2011)

dx.doi.org/10.1021/cr3000169 | Chem. Rev. 2012, 112, 4507−4540